

Article

Anti-Adipogenic Lanostane-Type Triterpenoids from the Edible and Medicinal Mushroom *Ganoderma applanatum*

Xing-Rong Peng^{1,2,†}, Qian Wang^{3,†}, Hai-Guo Su^{1,2}, Lin Zhou^{1,2}, Wen-Yong Xiong^{1,3,*}  and Ming-Hua Qiu^{1,2,*}

¹ State Key Laboratory of Phytochemistry and Plant Resources in West China, Kunming Institute of Botany, Chinese Academy of Sciences, Kunming 650201, China; pengxingrong@mail.kib.ac.cn (X.-R.P.); suhg@mail.sysu.edu.cn (H.-G.S.); zhoulun@mail.kib.ac.cn (L.Z.)

² University of the Chinese Academy of Sciences, Beijing 100049, China

³ Key Laboratory of Medicinal Chemistry for Natural Resource, Ministry of Education, Yunnan Provincial Center for Research & Development of Natural Products, School of Chemical Science and Technology, Yunnan University, Kunming 650091, China; 20210209@ynu.edu.cn

* Correspondence: xwy@ynu.edu.cn (W.-Y.X.); mhchiu@mail.kib.ac.cn (M.-H.Q.)

† These authors contributed equally to this work.

Abstract: Our previous research has shown that lanostane triterpenoids from *Ganoderma applanatum* exhibit significant anti-adipogenesis effects. In order to obtain more structurally diverse lanostane triterpenoids to establish a structure–activity relationship, we continued the study of lanostane triterpenoids from the fruiting bodies of *G. applanatum*, and forty highly oxygenated lanostane-type triterpenoids (1–40), including sixteen new compounds (1–16), were isolated. Their structures were elucidated using NMR spectra, X-ray crystallographic analysis, and Mosher’s method. In addition, some of their parts were evaluated to determine their anti-adipogenesis activities in the 3T3-L1 cell model. The results showed that compounds 16, 22, 28, and 32 exhibited stronger anti-adipogenesis effects than the positive control (LiCl, 20 mM) at the concentration of 20 μM. Compounds 15 and 20 could significantly reduce the lipid accumulation during the differentiation process of 3T3-L1 cells, comparable to the untreated group. Their IC₅₀ values were 6.42 and 5.39 μM, respectively. The combined results of our previous and present studies allow us to establish a structure-activity relationship of lanostane triterpenoids, indicating that the *A-seco*-23→26 lactone skeleton could play a key role in anti-adipogenesis activity.

Keywords: *Ganoderma applanatum*; lanostane triterpenoid; Mosher’s method; anti-adipogenesis activity; structure–activity relationship



Citation: Peng, X.-R.; Wang, Q.; Su, H.-G.; Zhou, L.; Xiong, W.-Y.; Qiu, M.-H. Anti-Adipogenic Lanostane-Type Triterpenoids from the Edible and Medicinal Mushroom *Ganoderma applanatum*. *J. Fungi* **2022**, *8*, 331. <https://doi.org/10.3390/jof8040331>

Academic Editors: Tao Feng and Frank Surup

Received: 22 February 2022

Accepted: 18 March 2022

Published: 22 March 2022

Publisher’s Note: MDPI stays neutral with regard to jurisdictional claims in published maps and institutional affiliations.



Copyright: © 2022 by the authors. Licensee MDPI, Basel, Switzerland. This article is an open access article distributed under the terms and conditions of the Creative Commons Attribution (CC BY) license (<https://creativecommons.org/licenses/by/4.0/>).

1. Introduction

Macro-fungi provide crucial food and medicinal resources [1]. *Tricholoma matsutake*, [2,3] *Lentinula edodes*, [4,5], and *Collybia albuminosa* [6] are delicious mushrooms which contain plentiful amino acids, fatty acids, vitamins, crude fiber, and protein. In addition, *Fomitopsis pinicola* (SW.) [7] Karst, *Inonotus obliquus* [8,9], *Phellinus igniarius* [10,11], *Ganoderma lucidum* [12,13], and *Ganoderma sinense* [14,15] have been used as edible and medicinal mushrooms for preventing and treating various diseases. The *Ganoderma* genus plays an important role in the history of Chinese medicine [16]. *Shennong’s Herbal Classics* recorded its traditional effects to include improving eyesight, strengthening muscles and bones, reinforcing kidney function, soothing the nerves, and prolonging the lifespan. *G. lucidum* and *G. sinense* have been registered in the *Chinese Pharmacopoeia* (2015 version). Meanwhile, *G. lucidum* was also included in the catalog of the latest edition of “Homology of medicine and Food” in 2020. Modern pharmacological research has further demonstrated that *Ganoderma* has a variety of pharmacological activities [17–21]. Thus, *Ganoderma* has great prospects in preventing and treating diseases.

Ganoderma applanatum, belonging to the genus *Ganoderma*, has traditionally been used to treat various chronic diseases, such as chronic hepatitis, immunological disorders, neurasthenia, arthritis, and nephritis [22]. Meanwhile, *G. applanatum* has been made into capsules and injections to cure chronic liver fibrosis and inflammation in a clinical setting [23–26]. *G. applanatum* is rich in chemical constituents, including polysaccharides, triterpenoids, meroterpenoids, alkaloids, and steroids. The majority of studies relating to it focus on the application and development of polysaccharides [23,27–31]. However, our previous research proved that highly oxygenated triterpenoids showed significant anti-adipogenesis activities [27,28]. In order to search for more active compounds to clarify the structure–activity relationship to lay the foundations for the discovery of lead compounds, we continued to investigate triterpenoids isolated from *G. applanatum* and 40 lanostane-type triterpenoids; of these (1–40), 16 were new compounds (1–16, Figure 1). Furthermore, their anti-adipogenesis effects were evaluated in the 3T3-L1 cell model, and their structure–activity relationship was established.

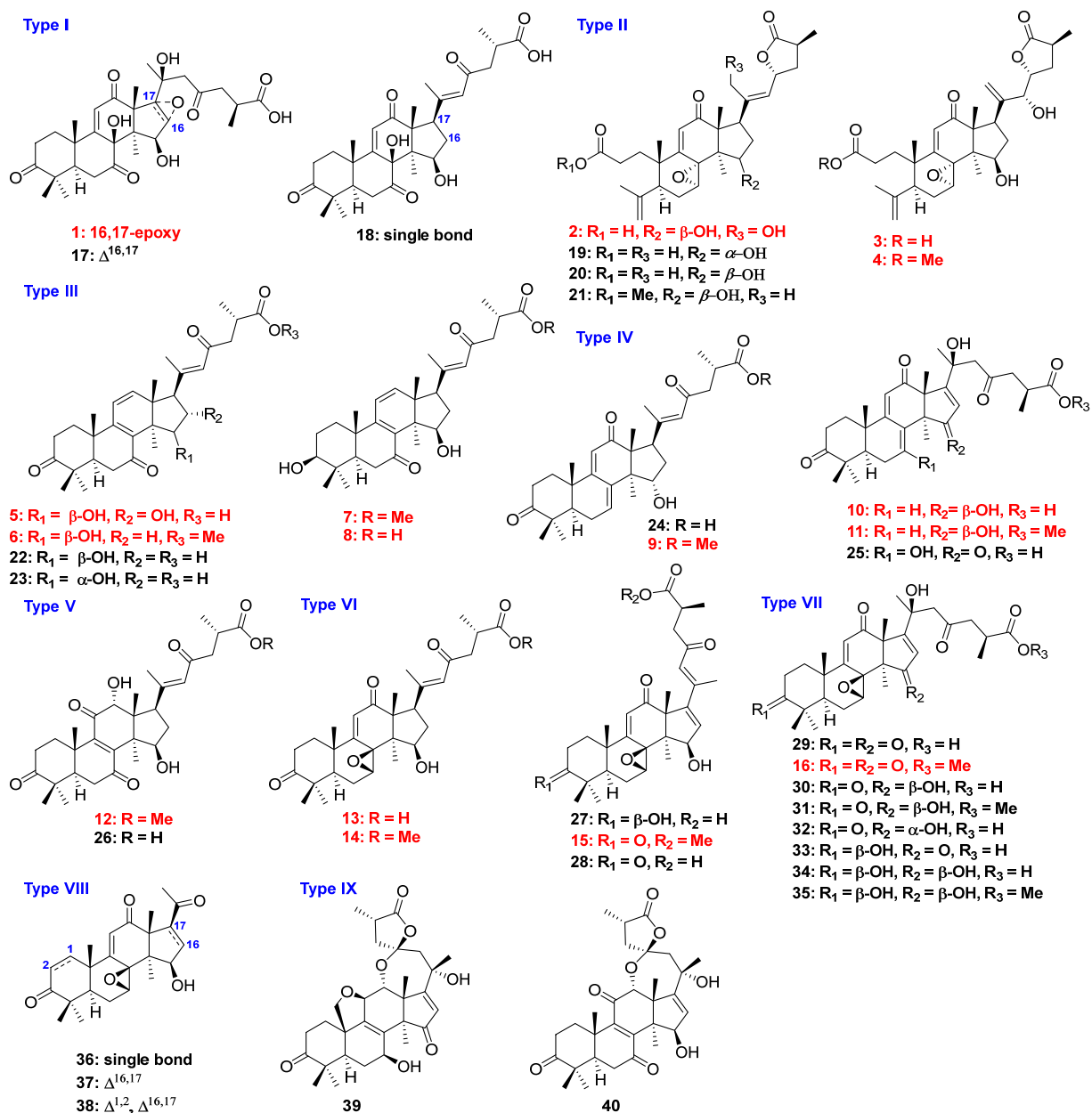


Figure 1. Structures and classifications of isolates from *G. applanatum* (red: new compounds).

2. Materials and Methods

2.1. General Experimental Procedures

NMR spectra were recorded on a Bruker AV-600 MHz (Bruker, Zurich, Switzerland) using TMS as an internal standard for chemical shifts with reference to the TMS resonance. ESIMS and HRTOF-ESIMS were measured on an API QSTAR Pulsar spectrometer. UV spectra were recorded on a Shimadzu UV-2401PC spectrometer. IR was recorded on the Bruker Tensor-27 instrument using KBr pellets. Optical rotations were recorded on a Horiba SEPA-300 polarimeter. CD spectra were measured on a Chirascan instrument. An Agilent 1100 series instrument equipped with an Agilent ZORBAX SB-C18 column (5 μ m, 9.6 mm \times 250 mm) was used for high-performance liquid chromatography (HPLC) separation.

TLC was performed on precoated TLC plates (200–250 μ m thickness, F254 Si gel 60, Qingdao Marine Chemical, Inc., Qingdao, China), with compounds visualized by spraying the dried plates with 10% aqueous H₂SO₄ followed by heating until they were dry. Silica gel ((200–300) mesh, Qingdao Marine Chemical, Inc.), Lichroprep RP-18 (40–63 μ m, Fuji), and Sephadex LH-20 (20–150 μ m, Pharmacia) were used for column chromatography. Methanol, chloroform, ethyl acetate, acetone, petroleum ether, n-hexane, and 2-propanol were purchased from Tianjing Chemical Reagents Co. (Tianjing, China). All other materials were of the highest grade available.

2.2. Fungal Materials

Ganoderma applanatum (39 kg) was purchased in December 2019 from a traditional Chinese medicine market in Kunming, Yunnan, China, which was identified by Prof. Yang Zhu-liang, Kunming Institute of Botany, Chinese Academy of Science (voucher No. 19122201).

2.3. Extraction and Isolation

G. applanatum (39 kg) was chipped and extracted with 95% EtOH under reflux three times (three hours each time). The combined EtOH extracts were evaporated under reduced pressure. The residue was suspended in H₂O and extracted with EtOAc. The volume of the combined EtOAc extracts was reduced to one-third under a reduced pressure. The residue was fractionated by macroporous resin (D-101; MeOH–H₂O, 50:50, 70:30, and 90:10, *v/v*): fractions I–III. Fraction III (245 g) was further fractionated by a silica gel column with petroleum ether (PE)/ethyl acetate (EA) as the mobile phase, which gave six subfractions (Fr. III-1 \rightarrow Fr. III-6).

Fr. III-2 (156 g) was treated by a silica gel column and CHCl₃/MeOH (80:1 \rightarrow 20:1, *v/v*) was used as an eluent. Ten fractions (Fr. III-2-1 \rightarrow Fr. III-2-10) were obtained, of which Fr. III-2-4 (20 g) was separated using Sephadex LH-20 (MeOH) to obtain three subfractions (Fr. III-2-4a \rightarrow Fr. III-2-4c). Compound **29** (235 mg) was purified through recrystallization from Fr. III-2-4b. The remaining solution was isolated using semi-preparative HPLC (CH₃CN/H₂O = 52%, *v/v*) to gain compound **6** (8 mg, *t_R* = 28.6 min). Fr. III-2-5 (10 g) was treated by a silica gel column, being eluted with PE/EA (20:1, *v/v*) to obtain five parts (Fr. III-2-5a \rightarrow Fr. III-2-5e). Subsequently, 5b and 5d were purified using P-TLC (CHCl₃/MeOH = 40:1, *v/v*) to obtain compounds **18** (11 mg), **16** (26 mg), and **21** (9.2 mg). Fr. III-2-6 (12 g) was separated by Rp-C18 with the elution of MeOH/H₂O (50% \rightarrow 55%) to obtain five fractions. Compounds **36** (6.2 mg) and **13** (12 mg) were obtained from Fr. III-2-6c and Fr. III-2-6d through P-TLC (CHCl₃/MeOH = 40:1, *v/v*), respectively.

Fr. III-2-7 (25 g) was fractionated by an Rp-C18 column, being eluted with MeOH/H₂O (50% \rightarrow 65% containing 0.3% CF₃COOH, *v/v*); nine subfractions (7a \rightarrow 7i) were obtained. Furthermore, 7d, 7g, and 7h were purified by semi-preparative HPLC (CH₃CN/H₂O = 45% \rightarrow 60%, *v/v*) to obtain compounds **14** (5.3 mg, *t_R* = 19.1 min), **4** (8.3 mg, *t_R* = 19.1 min), **8** (3.4 mg, *t_R* = 14.8 min), **9** (3.2 mg, *t_R* = 17.4 min), **12** (4.2 mg, *t_R* = 21.3 min), and **17** (5.1 mg, *t_R* = 22.2 min). Similarly, Fr. III-2-8 (31 g) was also treated using an Rp-C18 column with MeOH/H₂O (50% \rightarrow 55%) to obtain nine subfractions (8a \rightarrow 8i), from which compounds **37** (3.2 mg, *t_R* = 26.6 min), **38** (3.6 mg, *t_R* = 27.6 min), **31** (6.1 mg, *t_R* = 22.1 min), **22** (3.1 mg, *t_R* = 21.5 min), **25** (14 mg, *t_R* = 25.9 min), **19** (12.5 mg, *t_R* = 27.5 min), and **20** (7.2 mg,

$t_R = 20.7$ min) were purified by semi-preparative HPLC ($\text{CH}_3\text{CN}/\text{H}_2\text{O} = 43\% \rightarrow 60\%$ containing 0.3% CF_3COOH , v/v). The Rp-C18 column and semi-preparative HPLC were used to treat Fr. III-2-9 (20 g), and compounds **35** (2.5 mg, $t_R = 20.8$ min), **28** (2.9 mg, $t_R = 20.3$ min), **13** (2.1 mg, $t_R = 18.3$ min), **7** (2.2 mg, $t_R = 19.5$ min), and **23** (2.9 mg, $t_R = 18.5$ min) were isolated from 9d-1 and 9d-2. 9e (15 mg) was purified by P-TLC ($\text{CHCl}_3/\text{MeOH} = 30:1$, v/v) to obtain compounds **39** (4.2 mg) and **40** (2.8 mg).

The combination of Fr. III-4 and Fr. III-5 weighing 52 g was fractionated using Rp-C18 column elution with $\text{MeOH}/\text{H}_2\text{O}$ (35% \rightarrow 100%, v/v) to obtain six subfractions (Fr. III-4-1 \rightarrow Fr. III-4-6). Among these, Fr. III-4-2 \rightarrow Fr. III-4-5 were treated using Sephadex LH-20 (MeOH). Subsequently, the triterpenoid parts were purified by P-TLC ($\text{CHCl}_3/\text{MeOH} = 20:1$ containing 0.3% CF_3COOH , v/v) and semi-preparative HPLC ($\text{CH}_3\text{CN}/\text{H}_2\text{O} = 38\% \rightarrow 53\%$ containing 0.3% CF_3COOH , v/v) to obtain compounds **27** (4.2 mg), **24** (2.1 mg), **30** (6.2 mg), **5** (3.1 mg), **33** (3 mg), **26** (4.8 mg), **17** (5 mg, $t_R = 23.5$ min), **3** (7.2 mg, $t_R = 22.5$ min), **34** (6.1 mg, $t_R = 12.1$ min), **32** (3.3 mg, $t_R = 17.8$ min), **1** (3.0 mg, $t_R = 17.5$ min), **10** (2.9 mg), and **2** (3.7 mg).

Ganoapolic acid A (**1**): white powder (MeOH); $[\alpha]_D^{28} -1.2$ (c 0.25, MeOH); UV (MeOH); λ_{max} ($\log \epsilon$): 230 (3.36), and 196 (3.33); IR (KBr) ν_{max} 3428, 2953, 2943, 1653, 1636, 1423, 1364, 1212, and 1131 cm^{-1} ; ^1H NMR and ^{13}C NMR data: see Tables 1 and 2; HRMS (ESI-TOF) m/z : 561.2696 $[\text{M} + \text{H}]^+$ (calcd for $\text{C}_{30}\text{H}_{40}\text{O}_{10}$, 561.2694).

Table 1. ^1H NMR spectra of compounds 1–8 (600 MHz, methanol- d_4 , J in Hz, δ in ppm).

Position	1	2	3	4	5	6	7	8
1	1.87 dt (13.7 4.5) 2.21 dd (15.4 2.8)	1.86 m 2.20 m	1.82 m 2.16 m	1.85 m 2.17 m	1.91 m 2.29 m	1.87 m 2.16 m	2.02 m 1.51 m	1.50 m 2.02 m
2	2.40 m 2.95 m	2.19 m 2.36 m	2.17 m 2.34 m	2.25 m 2.40 m	2.55 m 2.74 m	2.51 m 2.71 m	1.78 m	1.77 m
3							3.24 t (8.4)	3.23 t (8.4)
5	1.74 dd (14.8 2.8)	2.97 t (8.3)	2.94 t (8.4)	2.95 dd (9.3 7.5)	2.28 m	2.19 m	1.66 dd (14.4 3.6)	1.66 dd (14.4 3.6)
6	2.30 dd (15.4 2.8) 3.30 m	2.03 m	1.99 m	2.03 m	2.44 dd (16.3 3.3)	2.52 m 2.66 m	2.62 m 2.48 m	2.48 m 2.59 m
7		4.93 s	4.95 s	4.98 s				
11	5.98 s	6.04 s	6.02 s	6.04 s	6.28 d (9.9)	6.14 d (10.2)	6.31 d (10.2)	6.31 d (10.2)
12					6.59 d (9.9)	6.59 d (10.2)	6.64 d (10.2)	6.65 d (10.2)
15	4.83 s	3.95 d (6.5)	3.91 d (6.5)	3.94 d (6.4)	4.20 s	4.44 d (7.8)	4.39 d (7.2)	4.39 d (7.2)
16	3.36 s	1.80 m 4.65 m	1.73 m 2.64 m	1.76 m 2.67 m	4.57 d (7.8)	2.20 m 2.42 m	2.16 m 2.51 m	2.16 m 2.51 m
17		3.33 m	3.21 dd (10.7 8.7)	3.23 m	2.73 m	2.73 m	2.87 m	2.83 m
18	1.97 s	1.30 s	1.37 s	1.39 s	0.99 s	1.01 s	1.00 s	0.99 s
19	1.65 s	1.01 s	1.04 s	1.05 s	1.14 s	1.27 s	1.16 s	1.16 s
21	1.34 s	4.37 s	5.33 s 5.39 s	5.36 s 5.43 s	1.21 s	2.23 s	2.19 s	2.19 s
22	2.66 d (14.9) 3.00 d (14.9)	5.78 d (8.6)	4.47 d (5.6)	4.50 d (5.6)	6.36 s	6.22 s	6.40 s	6.32 s
23		5.59 dd (8.6 6.6)	4.72 m	4.73 ddd (8.6 5.6 3.2)				
24	2.62 dd (18.3 5.6) 3.07 dd (18.3 7.7)	2.19 m	1.97 m 2.16 m	2.00 m 2.56 m	2.61 m 2.90 m	2.54 m 2.94 m	2.64 m 2.90 m	2.53 m 2.55 m
25	1.74 dd (14.8 2.8)	2.82 q (7.7)	2.84 m	2.86 m	2.74 m	2.97 m	2.85 m	2.84 m
26	1.16 d (6.6)	1.29 d (7.3)	1.22 d (6.5)	1.25 d (6.5)	1.18 d (7.0)	1.19 d (7.2)	1.17 d (7.2)	1.17 d (7.2)
28	1.14 s	4.80 s 4.98 s	4.77 s 4.95 s	4.77 s 4.95 s	1.12 s	1.13 s	1.00 s	1.00 s
29	1.07 s	1.80 s	1.78 s	1.80 s	1.10 s	1.14 s	0.90 s	0.90 s
30	0.74 s	1.06 s	1.01 s	1.04 s	1.10 s	0.94 s	0.95 s	0.95 s
OMe				3.65 s		3.68 s	3.65 s	

Table 2. ^{13}C NMR spectra of compounds 1–8 (150 MHz, methanol- d_4).

Position	1	2	3	4	5	6	7	8
1	37.6 CH ₂	37.7 CH ₂	37.7 CH ₂	37.5 CH ₂	36.5 CH ₂	35.6 CH ₂	36.3 CH ₂	36.3 CH ₂
2	35.1 CH ₂	30.4 CH ₂	30.5 CH ₂	30.5 CH ₂	35.0 CH ₂	34.0 CH ₂	28.1 CH ₂	28.1 CH ₂
3	215.8 C	177.4 C	177.4 C	175.6 C	217.1 C	214.3 C	78.3 CH	78.3 CH
4	48.7 C	146.5 C	146.5 C	146.3 C	51.9 C	46.9 C	39.7 C	39.8 C
5	48.5 CH	45.0 CH	45.3 CH	45.3 CH	50.7 CH	49.3 CH	50.8 CH	50.8 CH
6	35.8 CH ₂	28.2 CH ₂	28.1 CH ₂	28.1 CH ₂	37.5 CH ₂	36.8 CH ₂	37.0 CH ₂	37.0 CH ₂
7	205.9 C	64.7 CH	64.8 CH	65.0 CH	203.0 C	210.4 C	204.3 C	204.3 C
8	85.5 C	67.4 C	67.5 C	67.5 C	135.8 C	134.9 C	135.7 C	135.7 C
9	165.0 C	167.2 C	167.8 C	167.3 C	161.4 C	160.6 C	164.5 C	164.5 C
10	41.0 C	45.0 C	45.2 C	45.3 C	39.2 C	37.9 C	39.9 C	39.7 C
11	127.3 CH	130.7 CH	130.6 CH	130.6 CH	123.2 CH	122.0 CH	123.3 CH	123.3 CH
12	204.0 C	206.5 C	207.3 C	207.0 C	147.4 CH	147.5 CH	148.3 CH	148.3 C
13	62.3 C	60.8 C	60.4 C	60.4 C	52.2 C	50.2 C	51.4 C	51.4 C
14	47.0 C	54.4 C	54.4 C	54.4 C	48.0 C	52.5 C	53.9 C	53.8 C
15	80.0 CH	77.4 CH	77.2 CH	77.2 CH	84.9 CH	75.0 CH	76.5 CH	76.6 CH
16	61.2 CH	41.3 CH ₂	43.7 CH ₂	43.5 CH ₂	83.6 CH	36.2 CH ₂	37.2 CH ₂	37.2 CH ₂
17	71.4 C	43.3 CH	41.6 CH	41.6 CH	58.7 CH	48.5 CH	49.7 CH	49.7 C
18	24.6 CH ₃	20.2 CH ₃	20.2 CH ₃	20.2 CH ₃	19.2 CH ₃	17.1 CH ₃	20.2 CH ₃	21.2 CH ₃
19	19.9 CH ₃	24.2 CH ₃	23.4 CH ₃	23.4 CH ₃	21.1 CH ₃	19.5 CH ₃	18.0 CH ₃	18.0 CH ₃
20	73.4 C	144.1 C	148.7 C	148.7 C	156.5 C	157.3 C	158.8 C	158.4 C
21	27.8 CH ₃	61.8 CH ₂	117.6 CH ₂	117.5 CH ₂	19.7 CH ₃	21.4 CH ₃	21.4 CH ₃	21.3 CH ₃
22	53.9 CH ₂	130.8 CH	76.5 CH	76.5 CH	126.9 CH	124.8 CH	126.0 CH	126.4 CH
23	209.9 C	76.8 CH	80.9 CH	80.9 CH	200.8 C	198.3 C	200.6 C	201.3 C
24	48.7 CH ₂	38.3 CH ₂	32.2 CH ₂	32.2 CH ₂	48.7 CH ₂	47.7 CH ₂	48.8 CH ₂	49.0 CH ₂
25	35.8 CH	35.7 CH	35.3 CH	35.3 CH	36.2 CH	34.8 CH	36.6 CH	36.6 CH
26	17.4 CH ₃	15.9 CH ₃	16.3 CH ₃	16.0 CH ₃	17.5 CH ₃	17.1 CH ₃	17.4 CH ₃	17.7 CH ₃
27	179.7 C	182.7 C	183.1 C	183.2 C	179.7 C	176.4 C	178.1 C	180.8 C
28	22.3 CH ₃	115.9 CH ₂	115.9 CH ₂	115.9 CH ₂	21.0 CH ₃	25.6 CH ₃	27.8 CH ₃	27.8 CH ₃
29	24.9 CH ₃	23.5 CH ₃	23.4 CH ₃	23.4 CH ₃	25.9 CH ₃	20.4 CH ₃	15.7 CH ₃	15.7 CH ₃
30	30.7 CH ₃	21.3 CH ₃	21.4 CH ₃	21.4 CH ₃	19.7 CH ₃	20.6 CH ₃	21.2 CH ₃	20.2 CH ₃
OMe				52.3 CH ₃		51.8 CH ₃	52.3 CH ₃	

Ganoapptic acid B (2): white powder (MeOH); $[\alpha]_D^{28} +48.0$ (c 0.13, MeOH); UV (MeOH); λ_{\max} (log ϵ): 251 (3.75), and 196 (4.08); IR (KBr) ν_{\max} 3430, 2953, 2928, 1653, 1636, 1473, 1344, 1211, and 1147 cm^{-1} ; ^1H NMR and ^{13}C NMR data: see Tables 1 and 2; HRMS (ESI-TOF) m/z : 527.2653 $[\text{M} - \text{H}]^-$ (calcd for $\text{C}_{30}\text{H}_{40}\text{O}_8$, 527.2650).

Ganoapptic acid C (3): white powder (MeOH); $[\alpha]_D^{28} +42.0$ (c 0.09, MeOH); UV (MeOH); λ_{\max} (log ϵ): 251 (3.59), and 196 (3.93); IR (KBr) ν_{\max} 3423, 2955, 2930, 1673, 1635, 1428, 1380, 1219, and 1132 cm^{-1} ; ^1H NMR and ^{13}C NMR data: see Tables 1 and 2; HRMS (ESI-TOF) m/z : 527.2654 $[\text{M} - \text{H}]^-$ (calcd for $\text{C}_{30}\text{H}_{40}\text{O}_8$, 527.2650).

Methyl ganoapplate C (4): white powder (MeOH); $[\alpha]_D^{28} +39.5$ (c 0.07, MeOH); UV (MeOH); λ_{\max} (log ϵ): 251 (3.52), and 196 (3.85); IR (KBr) ν_{\max} 3458, 2957, 2928, 1689, 1606, 1473, 1375, 1210, and 1132 cm^{-1} ; ^1H NMR and ^{13}C NMR data: see Tables 1 and 2; HRMS (ESI-TOF) m/z : 565.2773 $[\text{M} + \text{Na}]^+$ (calcd for $\text{C}_{31}\text{H}_{42}\text{O}_8\text{Na}$, 565.2772).

Ganoapptic acid D (5): white powder (MeOH); $[\alpha]_D^{28} -20.1$ (c 0.21, MeOH); UV (MeOH); λ_{\max} (log ϵ): 242 (3.71), and 195 (3.79); IR (KBr) ν_{\max} 3503, 2967, 2935, 1663, 1635, 1452, 1390, 1200, and 1125 cm^{-1} ; ^1H NMR and ^{13}C NMR data: see Tables 1 and 2; HRMS (ESI-TOF) m/z : 511.2707 $[\text{M} - \text{H}]^-$ (calcd for $\text{C}_{30}\text{H}_{40}\text{O}_7$, 511.2701).

Methyl gibbosate M (6): white powder (MeOH); $[\alpha]_D^{28} -49.64$ (c 0.11, MeOH); UV (MeOH); λ_{\max} (log ϵ): 307 (3.21), 243 (3.80), and 196 (3.77); IR (KBr) ν_{\max} 3438, 2966, 2912, 1688, 1634, 1453, 1364, 1212, and 1132 cm^{-1} ; ^1H NMR and ^{13}C NMR data: see Tables 1 and 2; HRMS (ESI-TOF) m/z : 533.2873 $[\text{M} + \text{Na}]^+$ (calcd for $\text{C}_{31}\text{H}_{42}\text{O}_6\text{Na}$, 533.2874).

Methyl ganoapplate E (7): white powder (MeOH); $[\alpha]_D^{28} -69.3$ (c 0.13, MeOH); UV (MeOH); λ_{\max} (log ϵ): 316 (3.13), 243 (3.74), and 196 (3.72); IR (KBr) ν_{\max} 3413, 2953, 2916,

1657, 1620, 1454, 1374, 1209, and 1142 cm^{-1} ; ^1H NMR and ^{13}C NMR data: see Tables 1 and 2; HRMS (ESI-TOF) m/z : 535.3033 $[\text{M} + \text{Na}]^+$ (calcd for $\text{C}_{31}\text{H}_{44}\text{O}_6\text{Na}$, 535.3030).

Ganoaplic acid E (8): white powder (MeOH); $[\alpha]_D^{28}$ -143.5 (c 0.19, MeOH); UV (MeOH); λ_{max} ($\log \epsilon$): 317 (3.57), 244 (4.15), and 196 (4.05); IR (KBr) ν_{max} 3445, 2980, 2906, 1712, 1690, 1458, 1380, 1214, and 1028 cm^{-1} ; ^1H NMR and ^{13}C NMR data: see Tables 1 and 2; HRMS (ESI-TOF) m/z : 497.2911 $[\text{M} - \text{H}]^-$ (calcd for $\text{C}_{30}\text{H}_{41}\text{O}_6$, 497.2909).

Methyl gibbosate L (9): white powder (MeOH); $[\alpha]_D^{28}$ $+20.27$ (c 0.15, MeOH); UV (MeOH); λ_{max} ($\log \epsilon$): 291 (3.70), 244 (3.94), and 196 (3.85); IR (KBr) ν_{max} 3444, 2976, 2911, 1673, 1658, 1423, 1374, 1219, and 1140 cm^{-1} ; ^1H NMR and ^{13}C NMR data: see Tables 3 and 4; HRMS (ESI-TOF) m/z : 533.2876 $[\text{M} + \text{Na}]^+$ (calcd for $\text{C}_{31}\text{H}_{42}\text{O}_6\text{Na}$, 533.2874).

Ganoaplic acid F (10): white powder (MeOH); $[\alpha]_D^{28}$ $+20.86$ (c 0.14, MeOH); UV (MeOH); λ_{max} ($\log \epsilon$): 299 (3.77), and 196 (3.98); IR (KBr) ν_{max} 3437, 2953, 2924, 1678, 1656, 1433, 1374, 1215, and 1132 cm^{-1} ; ^1H NMR and ^{13}C NMR data: see Tables 3 and 4; HRMS (ESI-TOF) m/z : 511.2708 $[\text{M} - \text{H}]^-$ (calcd for $\text{C}_{30}\text{H}_{40}\text{O}_7$, 511.2701).

Methyl ganoapplate F (11): white powder (MeOH); $[\alpha]_D^{28}$ $+5.80$ (c 0.10, MeOH); UV (MeOH); λ_{max} ($\log \epsilon$): 301 (3.46), and 196 (3.87); IR (KBr) ν_{max} 3439, 2953, 2929, 1723, 1638, 1445, 1334, 1219, and 1138 cm^{-1} ; ^1H NMR and ^{13}C NMR data: see Tables 3 and 4; HRMS (ESI-TOF) m/z : 549.2827 $[\text{M} + \text{Na}]^+$ (calcd for $\text{C}_{31}\text{H}_{42}\text{O}_7\text{Na}$, 549.2823).

Table 3. ^1H NMR spectra of compounds 9–16 (600 MHz, J in Hz, δ in ppm).

Position	9 ^a	10 ^b	11 ^b	12 ^b	13 ^b	14 ^b	15 ^b	16 ^a
1	2.27 m 1.86 m	1.83 m 2.39 m	1.83 m 2.38 m	2.80 m 2.95 m	1.82 m 2.26 m	1.79 m 2.23 m	1.81 m 2.23 m	1.80 m 1.80 m
2	2.42 m 2.78 m	2.37 m 2.93 m	2.37 m 2.94 m	2.53 m 2.59 m	2.31 m 2.95 m	2.27 m 2.94 m	2.28 m 2.93 m	2.36 m 2.89 m
5	1.65 m	1.78 dd (12.8 3.1)	1.76 dd (11.4 3.60)	2.36 dd (15.0 3.0)	1.29 dd (12.4 5.9)	1.67 dd (12.6 6.0)	1.66 m	1.56 dd (12.66.0)
6	1.11 m 2.28 m	2.33 m 2.49 m	2.34 m 2.53 m	2.54 m 2.68 m	2.25 m	2.25 m	2.30 m	2.16 m
7	6.50 br s	6.62 m	6.63 d (7.2)		3.96 d (5.7)	3.93 d (5.4)	3.90 d (3.6)	4.45 d (5.4)
11	5.65 s	5.74 s	5.74 s		6.04 s	6.01 s	5.98 s	6.03 s
12				3.70 s				
15	4.58 t (8.3)	4.47 d (3.0)	4.47 d (3.0)	4.40 d (7.8)	4.08 d (6.0)	4.05 d (6.0)	4.35 d (3.0)	
16	1.80 m 2.48 m	5.75 d (3.0)	5.74 overlapped	2.07 m 2.43 m	1.94 m 2.43 m	1.91 m 2.42 m	6.20 d (3.0)	5.66 s
17	3.26 m			3.28 t (9.6)	3.24 dd (10.7 7.3)	3.21 dd (10.8 7.8)		
18	0.80 s	1.54 s	1.54 s	−0.096 s	1.46 s	1.43 s	1.90 s	1.76 s
19	1.28 s	1.39 s	1.40 s	1.31 s	1.47 s	1.45 s	1.47 s	1.44 s
20								
21	2.22 s	1.42 s	1.40 s	2.24 s	2.28 s	2.25 s	2.30 s	1.49 s
22	6.37 s	2.82 d (14.2) 3.01 d (14.2)	2.79 d (14.4) 2.79 dd (14.4)	6.31 s	6.56 s	6.52 s	6.50 s	2.92 d (15.0) 2.98 d (15.0)
24	2.54 m 2.94 m	2.66 dd (18.4 5.2) 3.02 m	2.79 dd (18.6 5.4) 3.02 dd (18.6 8.4)	2.54 m 2.94 m	2.62 m 2.92 m	2.62 m 2.88 m	2.58 m 2.93 m	3.04 m 2.59 dd (18.0 5.4)
25	2.93 m	2.80 m	2.81 m	1.19 m	2.89 m	2.89 m	2.89 m	2.89 m
26	1.17 d (6.7)	1.15 d (7.2)	1.13 d (7.2)	1.19 d (7.2)	1.20 d (7.0)	1.16 d (7.2)	1.20 d (7.0)	1.15 d (7.2)
28	1.11 s	1.20 s	1.20 s	1.15 s	1.09 s	1.09 s	1.10 s	1.11 s
29	1.15 s	1.11 s	1.06 s	1.13 s	1.13 s	1.13 s	1.38 s	1.12 s
30	1.08 s	1.06 s	3.63 s	1.24 s	0.96 s	0.96 s	1.00 s	1.28 s
OMe	3.68 s		3.56 s	3.69 s		3.65 s	3.63 s	3.65 s

^a Measured in CDCl_3 ; ^b measured in methanol- d_4 .

Table 4. ^{13}C NMR spectra of compounds 9–16 (150 MHz).

Position	9 ^a	10 ^b	11 ^b	12 ^b	13 ^b	14 ^b	15 ^b	16 ^a
1	35.6 CH ₂	36.7 CH ₂	36.8 CH ₂	35.1 CH ₂	38.4 CH ₂	38.4 CH ₂	38.4 CH ₂	37.2 CH ₂
2	34.2 CH ₂	35.4 CH ₂	35.4 CH ₂	34.3 CH ₂	34.9 CH ₂	34.9 CH ₂	34.8 CH ₂	33.8 CH ₂
3	214.8 C	217.2 C	217.2 C	214.9 C	216.4 C	216.4 C	216.5 C	213.6 C
4	47.0 C	48.4 C	48.8 C	47.1 C	48.7 C	48.5 C	48.8 C	47.8 C
5	49.5 CH	51.1 CH	51.2 CH	49.8 CH	50.7 CH	50.7 CH	51.2 CH	49.9 CH
6	23.9 CH ₂	25.2 CH ₂	25.2 CH ₂	37.6 CH ₂	22.6 CH ₂	22.6 CH ₂	22.4 CH ₂	21.6 CH ₂
7	130.9 CH	135.5 CH	135.5 CH	203.4 C	59.7 CH	59.7 CH	58.8 CH	57.1 CH
8	139.8 C	137.3 C	137.3 C	150.2 C	65.7 C	65.8 C	64.4 C	59.0 C
9	161.0 C	165.5 C	165.6 C	151.9 C	162.2 C	162.3 C	163.0 C	165.0 C
10	38.0 C	39.6 C	39.7 C	39.3 C	39.0 C	39.0 C	38.6 C	38.2 C
11	118.2 CH	118.3 CH	118.3 CH	203.9 C	127.6 CH	127.6 CH	127.2 CH	125.0 CH
12	202.5 C	206.5 C	206.5 C	79.6 CH	204.6 C	204.6 C	201.9 C	200.6 C
13	52.3 C	64.0 C	64.0 C	52.9 C	59.4 C	59.4 C	63.1 C	61.8 C
14	57.8 C	54.3 C	54.3 C	50.0 C	51.3 C	51.3 C	50.0 C	54.4 C
15	72.9 CH	79.3 CH	79.4 CH	77.5 CH	79.0 CH	79.0 CH	79.9 CH	202.7 C
16	36.5 CH ₂	127.5 CH	127.6 CH	34.2 CH ₂	38.2 CH ₂	38.2 CH ₂	134.9 CH	124.4 CH
17	45.7 CH	158.9 C	159.0 C	46.9 CH	49.6 CH	49.6 CH	148.8 C	181.9 C
18	17.8 CH ₃	29.0 CH ₃	29.1 CH ₃	18.6 CH ₃	20.3 CH ₃	20.3 CH ₃	27.0 CH ₃	30.9 CH ₃
19	21.3 CH ₃	21.5 CH ₃	21.5 CH ₃	19.0 CH ₃	21.0 CH ₃	21.0 CH ₃	21.2 CH ₃	20.8 CH ₃
20	157.6 C	72.6 C	72.6 C	157.5 C	159.0 C	159.2 C	156.0 C	72.6 C
21	20.4 CH ₃	29.0 CH ₃	29.1 CH ₃	20.3 CH ₃	21.5 CH ₃	21.5 CH ₃	17.5 CH ₃	29.1 CH ₃
22	125.7 CH	54.6 CH ₂	54.7 CH ₂	125.1 CH	127.5 CH	127.5 CH	127.1 CH	52.7 CH ₂
23	198.3 C	209.8 C	209.7 C	198.6 C	201.0 C	201.0 C	201.7 C	206.3 C
24	47.7 CH ₂	48.8 CH ₂	48.7 CH ₂	47.9 CH ₂	48.7 CH ₂	48.7 CH ₂	48.9 CH ₂	47.8 CH ₂
25	34.7 CH	35.8 CH	35.9 CH	35.0 CH	36.3 CH	36.3 CH	36.3 CH	34.5 CH
26	17.0 CH ₃	17.4 CH ₃	17.3 CH ₃	16.9 CH ₃	17.4 CH ₃	17.4 CH ₃	17.5 CH ₃	17.0 CH ₃
27	176.4 C	179.7 C	178.2 C	176.7 C	179.7 C	178.2 C	180.1 C	176.2 C
28	25.2 CH ₃	22.9 CH ₃	25.5 CH ₃	26.9 CH ₃	24.9 CH ₃	24.9 CH ₃	24.9 CH ₃	24.5 CH ₃
29	22.3 CH ₃	25.2 CH ₃	22.9 CH ₃	20.4 CH ₃	22.3 CH ₃	22.3 CH ₃	22.5 CH ₃	22.1 CH ₃
30	18.1 CH ₃	29.0 CH ₃	29.1 CH ₃	27.4 CH ₃	22.5 CH ₃	22.5 CH ₃	24.9 CH ₃	25.9 CH ₃
OMe	51.8 CH ₃		52.2 CH ₃	52.0 CH ₃		52.3 CH ₃	52.0 CH ₃	51.9 CH ₃

^a Measured in CDCl₃; ^b measured in methanol-*d*₄.

Methyl gannosate I (**12**): white powder (MeOH); $[\alpha]_D^{28} +95.0$ (*c* 0.14, MeOH); UV (MeOH); λ_{\max} (log ϵ): 249 (3.99), and 195 (3.73); IR (KBr) ν_{\max} 3452, 2985, 2921, 1673, 1618, 1425, 1376, 1221, and 1132 cm⁻¹; ¹H NMR and ¹³C NMR data: see Tables 3 and 4; HRMS (ESI-TOF) *m/z*: 565.2769 [M + Na]⁺ (calcd for C₃₁H₄₂O₈Na, 565.2772).

Ganoapptic acid G (**13**): white powder (MeOH); $[\alpha]_D^{28} -32.86$ (*c* 0.14, MeOH); UV (MeOH); λ_{\max} (log ϵ): 242 (3.99), and 196 (3.86); IR (KBr) ν_{\max} 3440, 2978, 2965, 1683, 1628, 1403, 1364, 1200, and 1151 cm⁻¹; ¹H NMR and ¹³C NMR data: see Tables 3 and 4; HRMS (ESI-TOF) *m/z*: 535.0000 [M + Na]⁺ (calcd for C₃₀H₄₀O₇Na, 535.0000).

Methyl ganoapplate G (**14**): white powder (MeOH); $[\alpha]_D^{28} +0.80$ (*c* 0.07, MeOH); UV (MeOH); λ_{\max} (log ϵ): 243 (3.79), and 196 (3.77); IR (KBr) ν_{\max} 3445, 2963, 2931, 1683, 1638, 1453, 1384, 1209, and 1142 cm⁻¹; ¹H NMR and ¹³C NMR data: see Tables 3 and 4; HRMS (ESI-TOF) *m/z*: 549.2823 [M + Na]⁺ (calcd for C₃₁H₄₂O₇Na, 549.2823).

Methyl applate C (**15**): white powder (MeOH); $[\alpha]_D^{28} +43.44$ (*c* 0.18, MeOH); UV (MeOH); λ_{\max} (log ϵ): 248 (3.99), and 196 (3.95); IR (KBr) ν_{\max} 3443, 2956, 2915, 1665, 1624, 1433, 1376, 1205, and 1132 cm⁻¹; ¹H NMR and ¹³C NMR data: see Tables 3 and 4; HRMS (ESI-TOF) *m/z*: 547.2672 [M + Na]⁺ (calcd for C₃₁H₄₀O₇Na, 547.2666).

Methyl gibbosate A (**16**): white powder (MeOH); $[\alpha]_D^{28} +18.94$ (*c* 0.15, MeOH); UV (MeOH); λ_{\max} (log ϵ): 237 (3.78), and 196 (3.82); IR (KBr) ν_{\max} 3430, 2953, 2929, 1703, 1628, 1433, 1354, 1229, and 1147 cm⁻¹; ¹H NMR and ¹³C NMR data: see Tables 3 and 4; HRMS (ESI-TOF) *m/z*: 563.2612 [M + Na]⁺ (calcd for C₃₁H₄₀O₈Na, 563.2615).

X-ray Crystallographic Data for *Ganoapptic acid A* (**1**): C₃₀H₄₀O₁₀·CH₄O·H₂O, *M* = 610.68, *a* = 13.9761(7) Å, *b* = 6.9089(3) Å, *c* = 15.8732(7) Å, α = 90°, β = 90.948(2)°, γ = 90°.

$V = 1532.50(12) \text{ \AA}^3$, $T = 100.(2) \text{ K}$, space group $P1211$, $Z = 2$, $\mu(\text{Cu K}\alpha) = 0.844 \text{ mm}^{-1}$, 26,208 reflections measured, 5973 independent reflections ($R_{int} = 0.0593$). The final R_1 values were 0.0504 ($I > 2\sigma(I)$). The final $wR(F^2)$ values were 0.1381 ($I > 2\sigma(I)$). The final R_1 values were 0.0543 (all data). The final $wR(F^2)$ values were 0.1436 (all data). The goodness of fit for F^2 was 1.042. Flack parameter = 0.07(9).

2.4. Mosher's Method

The specific esterification of compound **4** was performed based on the previous method [32]. The ^1H NMR spectroscopic data of the (*R*)-MTPA ester derivative (**4r**) of **4** (600 MHz, pyridine- d_5 ; data were obtained from the reaction NMR tube directly and assigned on the basis of correlations of the ^1H - ^1H COSY spectrum): δ 4.253 (1H, m, H-15), δ 2.158 (1H, m, H-16a), δ 2.756 (1H, m, H-16b), δ 3.566 (1H, m, H-17), δ 5.619 (1H, s, H-21a), δ 5.632 (1H, s, H-21b), δ 5.007 (1H, m, H-22), δ 5.067 (1H, m, H-23), δ 2.759 (1H, m, H-24a), δ 1.905 (1H, m, H-24b), δ 3.080 (1H, m, H-25), δ 1.198 (3H, s, Me-26). Meanwhile, the ^1H NMR spectroscopic data of the (*S*)-MTPA ester derivative (**4s**) of **4** were: δ 4.255 (1H, m, H-15), δ 2.156 (1H, m, H-16a), δ 2.756 (1H, m, H-16b), δ 3.568 (1H, m, H-17), δ 5.639 (1H, s, H-21a), δ 5.633 (1H, s, H-21b), δ 5.003 (1H, m, H-22), δ 5.062 (1H, m, H-23), δ 2.756 (1H, m, H-24a), δ 1.903 (1H, m, H-24b), δ 3.078 (1H, m, H-25), δ 1.196 (3H, s, Me-26) (see Figures S29–S31 in Section S10).

2.5. Inhibition of Lipogenesis Assay

2.5.1. Cell Culture and Adipocyte Differentiation

3T3-L1 cells were purchased from the American Type Culture Collection (ATCC, Manassas, VA, U.S.A.). The culture and differentiation of 3T3-L1 cells were performed based on the description reported previously [28]. Firstly, Dulbecco's modified Eagle's medium (DMEM) containing 10% bovine calf serum (CS) was used to cultivate 3T3-L1 cells. The whole system was incubated at 37 °C in a humidified atmosphere of 5% CO_2 and 95% air. Secondly, different medium systems were used for the different differentiated phases. Confluent cells were grown in DMEM medium containing 1 $\mu\text{g}/\text{mL}$ insulin, 1 μM dexamethasone (DEX), 0.5 mM 3-isobutyl-1-methylxanthine (IBMX), and 1 μM rosiglitazone (Rosi). Then, on the third day, post-differentiation medium—namely, DMEM with 10% fetal bovine serum (FBS) and 1 $\mu\text{g}/\text{mL}$ insulin—was used to continually cultivate the cells. From the fourth day, DMEM + 10% FBS was used as a maintenance medium for cell differentiation. In this process, it commonly takes two days for the mature adipocytes to form. During the whole differentiation process, the tested compounds or 0.1% DMSO were added to the differentiated 3T3-L1 cells, for which the 0.1% DMSO group was used as the vehicle.

2.5.2. Cell Viability Assay

The viability of cell treated with compounds **15** and **20** was determined by the MTS method. The detailed experimental procedures were similar to those described in our previous study [29].

2.5.3. Lipid Content Analysis

The intracellular lipid contents of 3T3-L1 adipocytes were determined by Oil Red O staining [33]. Briefly, differentiated 3T3-L1 cells were washed twice with PBS and fixed with 10% formaldehyde for 1 h. After another washing with PBS, the fixed cells were stained with 0.5% Oil Red O in 3:2 of Oil Red O/ H_2O for 15 min at room temperature and then washed with 60% isopropanol and distilled water. The lipid content was imaged with an inverted light microscope Nikon TS100 (Tokyo, Japan). Finally, 100% isopropanol was used to elute Oil Red O dye and it was quantified at 492 nm absorbance.

3. Results and Discussion

The molecular formula of ganoappic acid **1** was established to be $C_{30}H_{40}O_{10}$ by HRESIMS ion at m/z 561.2696 $[M + H]^+$ (calcd. 561.2694), suggesting 11 degrees of unsaturation. Its ^{13}C NMR spectra displayed 30 carbon resonances, of which seven methyls, three ketone carbonyls (δ_C 215.8, δ_C 205.9, and δ_C 209.9), an α,β -unsaturated carbonyl (δ_C 165.0, δ_C 127.3, and δ_C 204.0), one carboxyl (δ_C 179.7), two oxygenated methines (δ_C 80.0 and δ_C 61.2), and three quaternary carbons containing oxygen (δ_C 85.5, δ_C 71.4, and δ_C 73.4) were assigned based on the HSQC and ^{13}C -DEPT NMR spectra (see Figures S2 and S4 in Section S1). These data indicated that the structure of compound **1** was similar to that of gibbolic acid **G** with a 7,12,23-trioxo-8,20-dihydroxy-lanosta-9,11-en-26-oic acid skeleton [34], except for the presence of one oxygenated methine and one oxygenated quaternary carbon and the absence of a double bond at C-16 and C-17 in **1**. Furthermore, the HMBC spectrum (Figure 2A) of **1** revealed the correlations of H₃-21 with C-20 (δ_C 73.4), C-22, and the oxygenated quaternary carbon (δ_C 71.4); of H₃-30 with C-15 (δ_C 80.0); and of H-15 (δ_H 4.83, s) with the oxygenated methine (δ_C 61.2) and quaternary carbons (δ_C 71.4). Meanwhile, the proton of the methine containing oxygen (δ_H 3.36, s) showed the HMBC correlations with C-13, C-14, C-15, and C-20, as well as the 1H - 1H COSY correlation with H-15 (Figure 2A), which certified that C-16 and C-17 was substituted by hydroxyls. According to the molecular formula of **1**, an epoxy was present in **1** at C-16 and C-17.

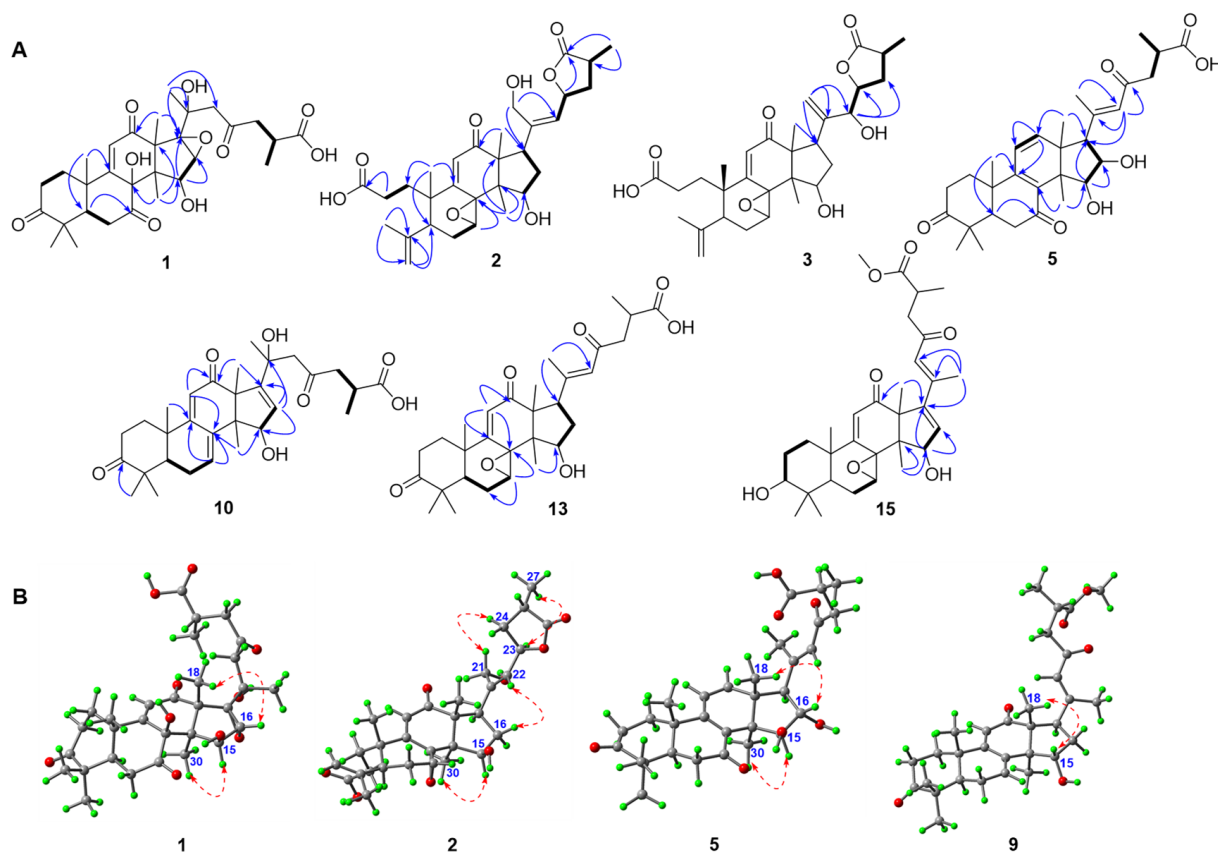


Figure 2. (A) Selected HMBC (H→C) and 1H - 1H COSY (H—H) correlations of compounds **1**–**3**, **5**, **10**, **13**, and **15**. (B) Selected ROESY correlations of compounds **1**, **2**, **5**, and **9**.

In the ROESY spectrum (Figure 2B) of **1**, H-15 showed an apparent cross peak with H₃-30, while H-16 correlated with H₃-18, suggesting that H-15 and H-16 were α - and β -oriented, respectively. The X-ray crystallographic analysis (Figure 3A) of **1** (Cu $\kappa\alpha$) further confirmed that the absolute configurations of C-15, C-16, C-20, and C-25 were *R*,

S, *S*, and *S* (see Table S1 in Section S1). Finally, the structure of **1** was determined to be (20*S*,25*S*)-7,12,23-trioxo-8 β ,20-dihydroxy-16 α ,17 α -epoxy-lanosta-9,11-en-26-oic acid.

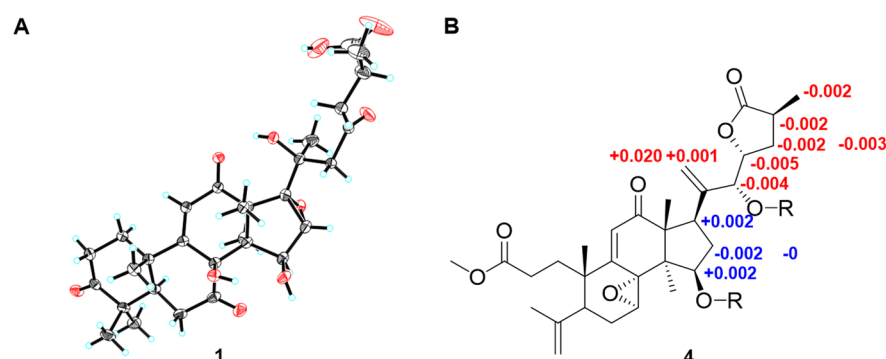


Figure 3. (A) X-ray crystallographic structure of **1**; (B) values of $\delta_S - \delta_R$ of the MTPA esters of **4**.

Ganoapptic acid B (**2**) was isolated as a colorless solid. Its molecular formula was determined to be $C_{30}H_{40}O_8$ by the HRESIMS. The 1D NMR and HSQC data of **2** supported the presence of five methyls, an α,β -unsaturated ketone, two carboxyl or ester carbonyls, one oxygenated methylene (δ_H 4.37, s; δ_C 61.8), three oxygenated methines (δ_H 3.95, d, $J = 6.5$ Hz, δ_C 77.4; δ_H 4.93, s, δ_C 64.7; δ_H 5.59, dd, $J = 8.6$ and 6.6 Hz, δ_C 76.8), one quaternary carbon containing oxygen (δ_C 67.4), a terminal double bond (δ_C 146.5; δ_C 115.9), and a double bond (δ_C 144.1; δ_H 5.78, d, $J = 8.6$ Hz, δ_C 130.8), which indicated that compound **2** was an *A*-*seco*-lanostane triterpenoid and had the similar structure to that of gibbolicolid F. [35] However, five methyls and an oxygenated methylene were observed in **2**, rather than the six methyls found in gibbolicolid F. The detailed analysis of the 2D NMR spectra (see Figures S10–S13 in Section S2) exhibited the long-range HMBC correlations (Figure 2A) of the oxygenated methylene with C-17, C-20, and C-22; of H₃-18 with C-12, C-13, C-14, and C-17; and of H-22 with C-17, C-20, C-23, and C-24, together with the ¹H-¹H COSY correlations of H-22/H-23/H₂-24/H-25/H₃-26. These pieces of evidence confirmed that the hydroxyl was connected to C-21.

The ROESY cross peaks (Figure 2B) of H-7/H₃-18 and H-15/H₃-30 demonstrated that both H-15 and the epoxy between C-7 and C-8 were α . H₂-21 showed a ROESY correlation with H-23, suggesting that the double bond at C-20 and C-22 was *Z*. In addition, H₃-26 displayed the ROESY correlation with H-23, hinting that H₃-26 and H-23 were on the same face. Moreover, the *dd*-peak type of H-23 ($J = 8.6$ and 6.6 Hz) was consistent with that of gibbolicolid B (δ_H 5.31, dd, $J = 13.2$ and 8.0 Hz), which further indicated that the absolute configurations of C-23 and C-25 were *R* and *S*, respectively. [35] Therefore, the structure of **2** was assigned as (23*R*,25*S*)-15 β ,21-dihydroxyl-7 α ,8 α -epoxy-12-oxo-3,4-*seco*-lanosta-4(28),9-(11),20*E*(22)-trien-23,26-olide-3-oic acid and named ganoapptic acid B (**2**).

The molecular formula of ganoapptic acid C (**3**) was established to be $C_{30}H_{40}O_8$ by the HRESIMS. The 1D NMR spectra (see Figures S15 and S16 in Section S6) of **3** showed a high similarity with those of ganoapptic acid B (**2**), suggesting that compound **3** was an *A*-*seco* lanostane triterpenoid. However, the comparison of the 1D NMR spectroscopic data of **2** and **3** revealed that another terminal double bond (δ_C 117.6 and δ_C 148.7) and oxygenated methine (δ_C 76.5) were present in **3**, while a double bond (C-20–C-22) and an oxygenated methylene (C-21) were observed in **2**. Furthermore, the obvious ¹H-¹H COSY correlations of H₃-26/H-25/H₂-24/H-23/H-22, as well as the HMBC correlations of H₃-26 with C-24, C-25, and C-27 and of H₂-24 with C-22, C-23, and C-26, indicated that the hydroxyl was located at C-22 (Figure 2A). Meanwhile, H-22 (δ_H 4.47, d, $J = 5.6$ Hz) and H-17 displayed HMBC correlations of the terminal double bond, proving that the terminal double bond was at C-21 and C-20.

The 1D NMR spectra and molecular weight (see Figures S22 and S23 in Section S8, and Figure S28 in Section S9) of methyl ganoapplate C (**4**) showed that compound **4** was the ester derivative of **3**, which was confirmed by the HMBC correlation of OMe

with C-27 (δ_C 175.6). The analysis of the ROESY spectra of **3** and **4** exhibited cross peaks of H-7/H₃-18, H-23/H₃-26, and H-22/H-25, indicating that the epoxy between C-7 and C-8 was α ; meanwhile, H-23 and H₃-26 were cofacial (Figure 2B). Biogenetically, the absolute configuration of C-25 from *G. applanatum* was S. Thus, C-23 was determined to be R. The absolute configuration of C-22 was established as R based on the revised Mosher's method (Figure 3B) [33]. Thus, the structures of **3** and **4** were elucidated as (22R,23R,25S)-15 β ,22-dihydroxyl-7 α ,8 α -epoxy-12-oxo-3,4-*seco*-lanosta-4(28),9(11),20(21)-trien-23,26-olide-3-oic acid and methyl (22R,23R,25S)-15 β ,22-dihydroxyl-7 α ,8 α -epoxy-12-oxo-3,4-*seco*-lanosta-4(28),9(11),20(21)-trien-23,26-olide-3-oate, respectively.

Ganoaplic acid D (**5**) was isolated as a white powder and its molecular formula was determined to be C₃₀H₄₀O₇ based on the HRESIMS at m/z 511.2701 [M – H][–] (calcd. 511.2707). Its ¹³C-DEPT spectra (see Figures S32 and S33 in Section S11) showed thirty carbon resonances belonging to seven methyls, four methylenes, eight methines (including three *sp*² and two oxygenated), and eleven quaternary carbons (including three ketone carbonyls, one carboxyl, and three *sp*²). These data indicated that compound **5** was a lanostane-type triterpenoid and had similar structure to that of gibbolic acid M (**22**) [35], except for the replacement of the methylene (C-16) in **22** with an oxygenated methine in **5**. The HMBC spectrum of **5** revealed the correlations of H₃-30 with C-15 (δ_C 84.9), C-13, and C-14; of H₃-18 with C-12, C-13, C-14, and C-17; and of H-17 with C-16, C-15, C-20, C-21, and C-22, suggesting that C-16 was an oxygenated methine in **5**, together with the ¹H-¹H COSY correlations of H-15/H-16/H-17 (Figure 2A). The ROESY correlations of H-15/H₃-30 and of H-16/H₃-18 illustrated that H-15 and H-16 were α - and β -oriented, respectively. The *E*-configuration of $\Delta^{20,22}$ was determined by the ROESY correlation of H-22/H-17/H-16. Therefore, the structure of **5** was assigned as 15 β ,16 α -dihydroxy-3,7,23-trioxolanosta-8,11,20*E*(22)-trien-26-oic acid and named ganoaplic acid D (**5**).

Methyl gibbosate M (**6**) had the molecular formula of C₃₁H₄₂O₆ based on the positive HRESIMS at m/z 533.2874 [M + Na]⁺ (calcd. 533.2873). The 1D NMR spectra (see Figures S39 and S40 in Section S13) of **6** were the same as those of gibbolic acid M (**22**) [35], except that the carboxyl at C-27 in **22** was replaced by the ester carbonyl in **6**. The key HMBC correlation of OMe with C-27 confirmed the above deduction. The characteristic *d*-coupling type of H-15 and the ROESY correlation of H-15/H₃-30 indicated that the 15-OH was β -oriented [35]. Finally, the structure of **6** was established to be methyl 15 β -hydroxy-3,7,23-trioxolanosta-8,11,20*E*(22)-trien-26-oate and named methyl gibbosate M (**6**).

Methyl ganoaplate E (**7**) was isolated as a white powder and its molecular formula was determined to be C₃₁H₄₄O₆ by the HRESIMS. The analysis of the 1D NMR spectra (see Figures S46 and S47 in Section S15) of **7** showed that compound **7** had a similar structure to that of **6**, with the only difference being in the replacement of the ketone carbonyl at C-3 in **6** with the oxygenated methine in **7**, which was confirmed by the HMBC correlations of H₃-28, H₃-29, and H-5 with the oxygenated methine (δ_C 78.3). The ROESY correlations of H-3/H-5 and of H-15/H₃-30 indicated that 3-OH and 15-OH were β .

Ganoaplic acid E (**8**) was deduced to be the demethylated derivative of **7** on the basis of the HMBC correlation regarding the lack of the OMe at C-27 and the low-field shift of C-27. Thus, the structures of compounds **7** and **8** were elucidated as methyl (25S)-3 β ,15 β -dihydroxy-7,23-dioxolanosta-8,11,20*E*(22)-trien-26-oate and (25S)-3 β ,15 β -dihydroxy-7,23-dioxolanosta-8,11,20*E*(22)-trien-26-oic acid, respectively.

Methyl gibbosate O (**9**) was found to be similar to the known compound gibbolic acid O (**24**) [35] based on the 1D NMR spectroscopic data, except for distinct differences in the chemical shift of C-27 and the presence of an additional methoxyl. The HMBC spectrum of **9** showed the correlation of OMe with C-27, suggesting that **9** was a methyl ester derivative of gibbolic acid O (**24**). Therefore, the structure of **9** was determined to be methyl 15 α -hydroxy-3,12,23-trioxolanosta-7,9(11),20*E*(22)-trien-26-oate.

The molecular formula of ganoaplic acid F (**10**) was deduced to be C₃₀H₄₀O₇ based on the HRESIMS and NMR data. Its 1D NMR spectra (see Figures S67 and S68 in Section S21) showed a similar tetracyclic skeleton to that of gibbolic acid O (**24**) [35] with a 15-hydroxy-

3,12-dioxolanosta-7(8),9(11)-diene skeleton, which was confirmed by the 2D NMR spectra. In addition, an oxygenated quaternary carbon signal (δ_C 72.6) and two sp^2 carbon signals (δ_C 127.5 and δ_C 158.9) were characteristic for the quaternary carbon containing oxygen at C-20 and the double bond at C-16 and C-17. Furthermore, the HMBC correlations (Figure 2A) of H₃-30 with C-15; of H-15 with C-16 and C-17; of H₃-18 with C-17; of H₃-21 with C-17, C-20, and C-22; and of H-22 with C-20, C-23, and C-24 confirmed the above deduction.

Methyl ganoapplate F (**11**) was an ester derivative at C-27 of ganoaplic acid H (**10**), according to the HMBC correlation of OMe with C-27. The ROESY spectra of **10** and **11** showed cross peaks of H-15/H₃-30, indicating the β -orientation of 15-OH. Therefore, the structures of **10** and **11** were determined to be 15 β ,20-dihydroxy-3,12, 23-trioxo-5 α -lanosta-7,9(11),16-trien-26-oic acid and methyl 15 β ,20-dihydroxy-3,12,23-trioxo-5 α -lanosta-7,9(11),16-trien-26-oate, respectively.

Based on the NMR data analysis, methyl gibbosate I (**12**) was found to be close to that of **26** [35], with a 12,15-dihydroxy-3,7,11,23-tetraoxolanosta-8,20(22)-dien structure. The 2D NMR spectra further confirmed its structure and **12** had an additional methoxyl at C-27, which was proven by the key HMBC correlation of OMe with C-27. Moreover, the ROESY correlations of H-12/H₃-18 and H-15/H₃-30 demonstrated that 12-OH was α while 15-OH was β . Thus, the structure of **12** was deduced to be methyl 12 α ,15 β -dihydroxy-3,7,11,23-tetraoxolanosta-8,20(22)-dien-26-ate.

Ganoaplic acid G (**13**) was isolated as a white powder and its molecular formula was determined to be C₃₀H₄₀O₇ based on the HRMS (ESI-TOF) m/z 535.0000 [M + Na]⁺ (calcd. 535.0000). The 1D NMR spectra of **13** showed the presence of the ketone carbonyl at C-3, 7,8-epoxyl, α,β -unsaturated ketones (C-9/C-11/C-12 and C-20/C-22/C-23), 15-OH, and 27-oic acid, which was further confirmed by the 2D NMR spectra (Figure 2A). The aforementioned information indicated that compound **13** had the same planar structure as gibbosic acid N. [35] The comparison of the ROESY spectra of **13** and gibbosic acid N revealed that they were 15-isomers due to the existence of the ROESY correlation of H-15/H₃-30 and the d -coupling of H-15 [35]. Therefore, the structure of **13** was established to be 15 β -hydroxy-7 β ,8 β -epoxy-3,12,23-trioxolanosta-9(11),20E(22)-dien-26-oic acid. In addition, methyl ganoapplate G (**14**) was deduced to be the methylation product of **13** on the basis of the HMBC correlation of OMe with C-27.

Methyl applanate C (**15**) was found to have a similar structure to methyl ganoapplate F (**14**), except for the presence of a double bond in **15**, rather than one methylene and one methine in **14**. Furthermore, in the HMBC spectrum of **15**, the correlations (Figure 2A) of H₃-30 with C-15, of H-15 with the sp^2 methine and quaternary carbon, and of H₃-18 and H₃-21 with the sp^2 quaternary carbon were observed, which proved that the double bond was located at C-16 and C-17. The ROESY correlation of H-16/H₃-21 and H₃-18/H-22 suggested that the geometry of the 16,20(22)-conjugated diene was 17,20-Z-(16Z, 20E). Additionally, the ROESY correlation of H₃-30/H-15 demonstrated that 15-OH was β . Finally, the structure of **15** was determined to be methyl 15 β -hydroxy-7 β ,8 β -epoxy-3,12,23-trioxolanosta-9(11),16Z,20E(22)-trien-26-oate and named methyl applanate C (**15**).

Methyl gibbosate A (**16**) was considered to be the methylation derivative of gibbosic acid A (**29**) [34] because of their similar 1D and 2D spectra (see Figures S104–S109 in Section S33) and the HMBC correlation of OMe with C-27. 7 β ,8 β -epoxy was proven by the ROESY correlation of H-17/H₃-30. Thus, the structure of **16** was established to be methyl 20-hydroxy-7 β ,8 β -epoxy-3,12,15,23-tetraoxo-lanosta-9,16-dien-26-oate.

In addition, 24 known compounds were identified by comparing their 1D NMR spectra with those reported in the literature, and they were assigned as gibbosic acid G (**17**) [34], applanic acid B (**18**) [36], gibbosicolid E (**19**) [35], gibbosicolid F (**20**) [35], gibbosicolid G (**21**) [35], gibbosic acid M (**22**) [35], gibbosic acid L (**23**) [35], gibbosic acid O (**24**) [35], applanic acid D (**25**) [36], gibbosic acid I (**26**) [35], ganodapplanic acid D (**27**) [27], applanic acid C (**28**) [36], ganoapplanic acid F (**29**) [37], elfvingic acid B (**30**) [37], applanoxidic acid G methyl ester (**31**) [37], gibbosic acid C (**32**) [34], gibbosic acid B (**33**) [34], elfvingic acid C (**34**) [38], methyl ganoap-

planiate D (35) [37], applanone E (36) [36], ganoapplanoid K (37) [28], ganoapplanoid L (38) [28], ganoapplanilactone B (39) [37], and ganoapplanilactone A (40) [37].

Parts of the isolated compounds were evaluated to determine their anti-adipogenesis activities. At a concentration of 20 μM , compounds 16, 22, 28, and 32 showed comparable inhibition for lipid accumulation compared to the positive control (LiCl, 20 mM). Meanwhile, compounds 15 and 20 displayed stronger inhibitory effects than the positive control, even resembling the untreated group (Figure 4). Furthermore, compounds 15 and 20 did not show any toxicity for the 3T3-L1 cells when the concentration was less than 100 μM . At the concentrations of 1.25, 2.5, 5, 10, 20, and 30 or 40, compounds 15 and 20 showed significantly inhibitory activities in a dose-dependent manner, with IC_{50} values of 6.42 and 5.39 μM , respectively (Figure 5).

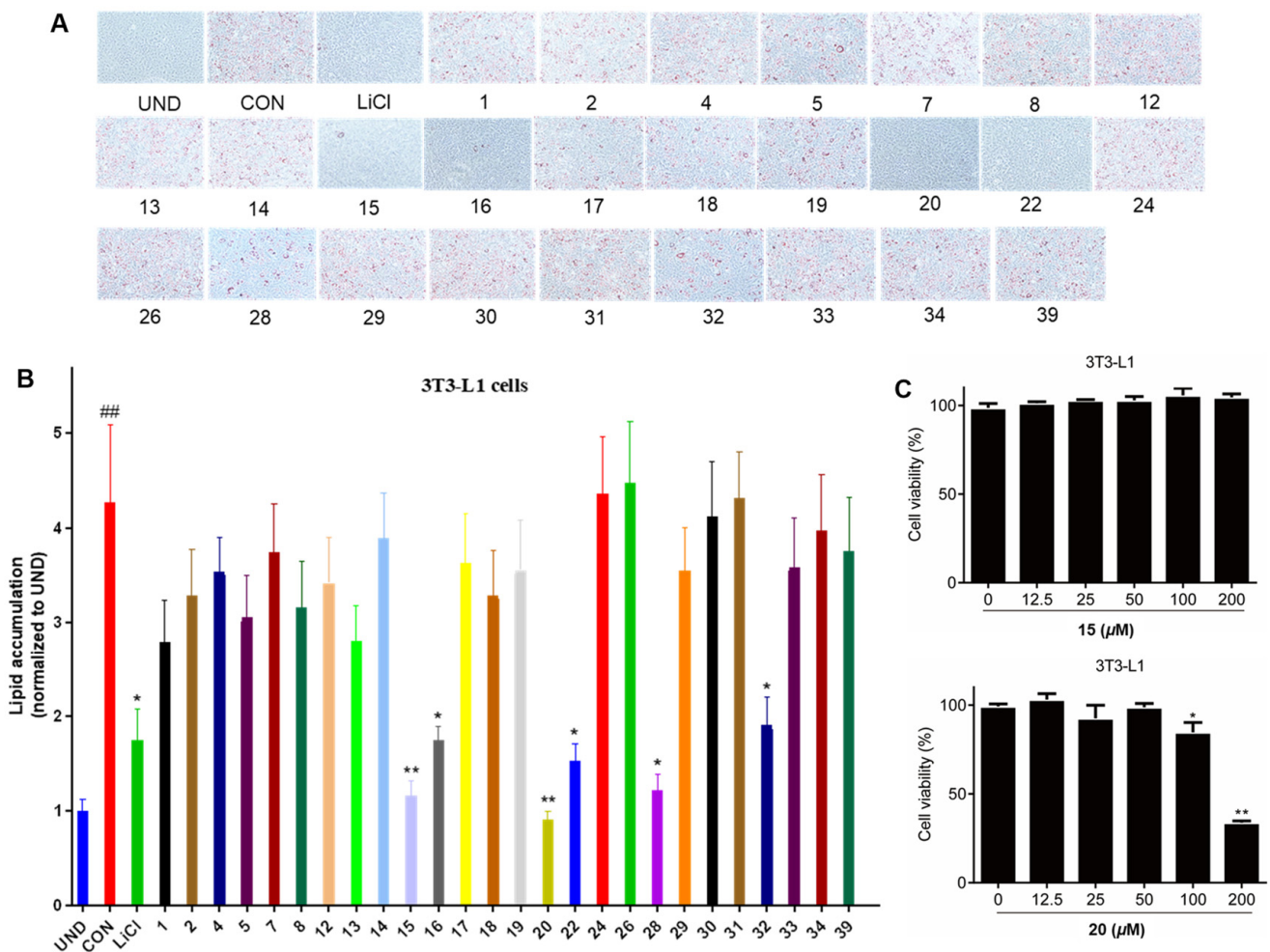


Figure 4. Effects of compounds (1, 2, 4, 5, 7, 8, 12–20, 22, 24, 26, 28–34, and 39) at a level of 20 μM on lipid accumulation during 3T3-L1 adipocyte differentiation (A). LiCl (20 mM) was used as a positive control. Quantification of intracellular lipids in Oil Red O-stained adipocytes (B). Cell viability of compounds 15 and 20 on 3T3-L1 pre-adipocytes when treated for 24 h with an MTS assay (C). Data are representative results from three independent experiments. Data are shown as mean \pm SD ($n = 3$) versus undifferentiated cells (UND). (##) $p < 0.01$ versus undifferentiated cells (UND). (*) $p < 0.05$ and (**) $p < 0.01$ versus fully differentiated cells (CON).

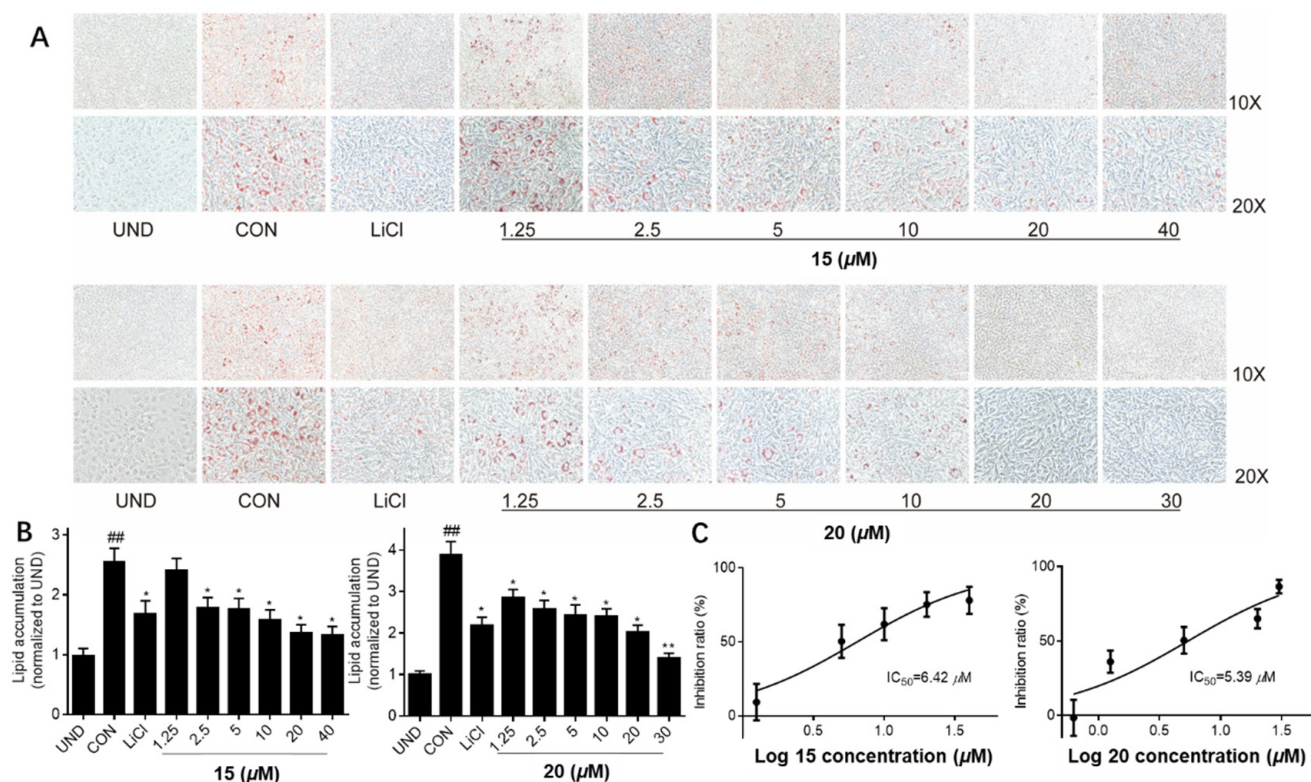


Figure 5. Effects of compounds 15 and 20 on lipid accumulation in 3T3-L1 adipocytes. (A) Oil Red O staining of cells administered with serial doses of compounds 15 and 20. (B) Quantification of intracellular lipid in Oil Red O-stained adipocytes. (C) The IC₅₀ values of compounds 15 and 20. LiCl (20 mM) was used as a positive control. Data are representative results from three independent experiments. Data are shown as mean ± SD ($n = 3$), versus undifferentiated cells (UND). (##) $p < 0.01$ versus undifferentiated cells (UND). (*) $p < 0.05$ and (**) $p < 0.01$ versus fully differentiated cells (CON).

The structures of the isolates were divided into nine types, including type I with a 7,12-dioxo-8-hydroxy-9,11-en fraction, type II with a A-seco-7,8-epoxy-9,11-en-12-oxo-23→27 lactone fraction, type III with a 7,23-dioxo-8(9),11(12),20(22)-trien fraction, type IV with a 12-oxo-7(8),9(11)-dien fraction, type V with a 7,11-dioxo-12-hydroxy-8(9)-en fraction, type VI with a 7,8-epoxy-12,23-dioxo-9(11),16(17),20(22)-trien fraction, type VII with a 20-hydroxy-7,8-epoxy-12,23-dioxo-9(11)-en fraction, type VIII with a 12-oxo-7,8-epoxy-9(11)-en-21,22,23,24,25,26,27-norlanostane, and type IX with a 12,23-epoxy-23→27 lactone fraction. The combined results of the previous and present studies showed that bioactive compounds were mainly present in type II (20 and 21), type III (22), type VI (15 and 28), type VII (16 and 32), and type VIII (37). For type II, when the relative configuration of 15-OH was α , the activity was decreased, similar to compound 19, while any changes in the side chain decreased their activities, such as compounds 2–4. For type III, no matter which reactions happened in type III, compounds 5–8 and 23 did not show inhibitory activity. For type VI, compound 27 was the 3-OH analogue of 15 and 28, leading to a decrease in inhibition. In type VII, the carbonyl at C-3 and the carbonyl or hydroxyl at C-15 could be the crucial active functionalities. C24 lanostane triterpenoids possessing a double bond at C-16 and C-17 displayed anti-adipogenesis activity [27,28]. Compared to the other compounds, compound 20 belonging to type II showed the strongest inhibitory activity, suggesting that A-seco-15 β -hydroxy-7,8-epoxy-12-oxolanosta-9,11-en-23→27 lactone could play a significant role in the anti-adipogenesis effect (Figure 6).

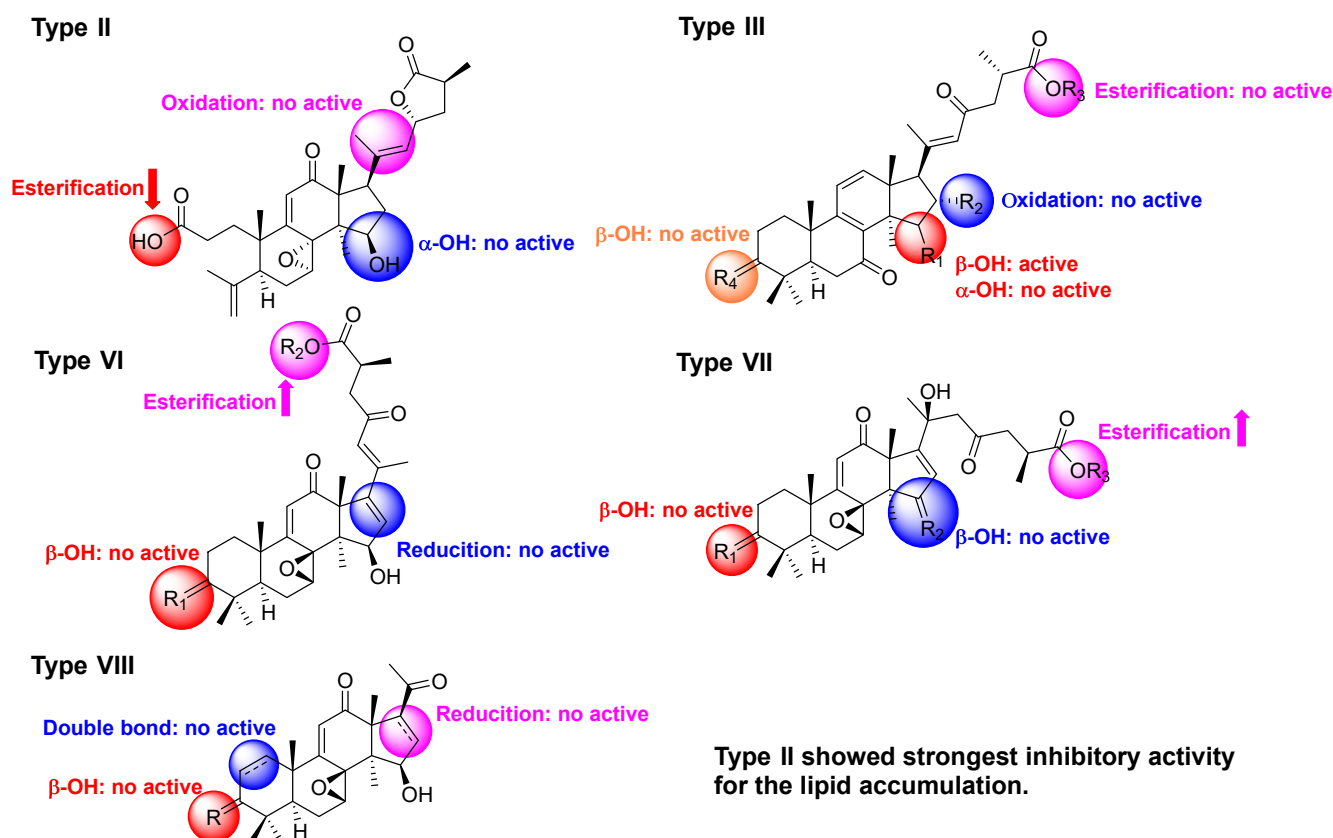


Figure 6. The proposed structure–activity relationship of triterpenoids from *G. applanatum*.

4. Conclusions

Overall, inspired by our previous studies, we investigate the lanostane-type triterpenoids of *G. applanatum*; 40 triterpenoids, including 16 new compounds, were isolated. Their anti-adipogenesis activities were evaluated and the results showed that compounds **15** and **20** can significantly inhibit lipid accumulation, with the IC_{50} values of 6.42 and 5.39 μ M, respectively. Furthermore, we established a structure–activity relationship for the lanostane-type triterpenoids from *G. applanatum*, suggesting that the structure skeleton (*A-seco*-15 β -hydroxy-7,8-epoxy-12-oxolanosta-9,11-en-23 \rightarrow 27 lactone) could be of importance for the anti-adipogenic effect. In the next step, we can use type III as a template for further structural modification in order to find the lead compound.

Supplementary Materials: The following supporting information can be downloaded at: <https://www.mdpi.com/article/10.3390/jof8040331/s1>, Section S1: 1D and 2D NMR spectra of compound **1**; Section S2: HRESIMS spectrum of **1**; Section S3: X-ray crystallographic data of **1**; Section S4: 1D and 2D NMR spectra of **2**; Section S5: HRESIMS spectrum of **2**; Section S6: 1D and 2D NMR spectra of **3**; Section S7: HRESIMS spectrum of **3**; Section S8: 1D and 2D NMR spectra of **4**; Section S9: HRESIMS spectrum of **4**; Section S10: Comparison of 1H NMR and 1H - 1H COSY spectra between **4r** and **4s**; Section S11: 1D and 2D NMR spectra of **5**; Section S12: HRESIMS spectrum of **5**; Section S13: 1D and 2D NMR spectra of **6**; Section S14: HRESIMS spectrum of **6**; Section S15: 1D and 2D NMR spectra of **7**; Section S16: HRESIMS spectrum of **7**; Section S17: 1D and 2D NMR spectra of **8**; Section S18: HRESIMS spectrum of **8**; Section S19: 1D and 2D NMR spectra of **9**; Section S20: HRESIMS spectrum of **9**; Section S21: 1D and 2D NMR spectra of **10**; Section S22: HRESIMS spectrum of **10**; Section S23: 1D and 2D NMR spectra of **11**; Section S24: HRESIMS spectrum of **11**; Section S25: 1D and 2D NMR spectra of **12**; Section S26: HRESIMS spectrum of **12**; Section S27: 1D and 2D NMR spectra of **13**; Section S28: HRESIMS spectrum of **13**; Section S29: 1D and 2D NMR spectra of **14**; Section S30: HRESIMS spectrum of **14**; Section S31: 1D and 2D NMR spectra of **15**; Section S32: HRESIMS spectrum of **15**; Section S33: 1D and 2D NMR spectra of **16**; Section S34: HRESIMS spectrum of **16**.

Author Contributions: Conceptualization, X.-R.P. and M.-H.Q.; methodology, Q.W., X.-R.P., H.-G.S., W.-Y.X. and M.-H.Q.; resources, X.-R.P., L.Z., W.-Y.X. and M.-H.Q.; data curation, X.-R.P. and Q.W.; writing—original draft preparation, X.-R.P.; writing—review and editing, X.-R.P., W.-Y.X. and M.-H.Q.; project administration, X.-R.P.; funding acquisition, X.-R.P. All authors have read and agreed to the published version of the manuscript.

Funding: This research was funded by the Basic Research Project of Yunnan Province (201901T070239) and the Youth Innovation Promotion Association of CAS (2019383).

Institutional Review Board Statement: Not applicable.

Informed Consent Statement: Not applicable.

Data Availability Statement: X-ray crystallographic data of **1** (CIF) are available free of charge.

Acknowledgments: This work was supported by grants from the Basic Research Program of Yunnan Province (202001AT070070), and the Youth Innovation Promotion Association of CAS (2019383). The authors are grateful to the Analytical and Testing Center at Kunming Institute of Botany for the NMR and ECD data collection.

Conflicts of Interest: The authors declare no conflict of interest. The funders had no role in the design of the study; in the collection, analysis, or interpretation of data; in the writing of the manuscript; or in the decision to publish the results.

References

1. Sudheer, S.; Bai, R.G.; Muthoosamy, K.; Tuvikene, R.; Gupta, V.K.; Manickam, S. Biosustainable production of nanoparticles via mycogenesis for biotechnological applications: A critical review. *Environ. Res.* **2022**, *204*, 111963–111979. [[CrossRef](#)] [[PubMed](#)]
2. Li, M.; Lv, R.; Xu, X.; Ge, Q.; Lin, S. *Tricholoma matsutake*-Derived Peptides Show Gastroprotective Effects against Ethanol-Induced Acute Gastric Injury. *J. Agric. Food Chem.* **2021**, *69*, 14985–14994. [[CrossRef](#)] [[PubMed](#)]
3. Li, M.; Ge, Q.; Du, H.; Lin, S. *Tricholoma matsutake*-derived peptides ameliorate inflammation and mitochondrial dysfunction in RAW264.7 macrophages by modulating the NF- κ B/COX-2 pathway. *Foods* **2021**, *10*, 2680. [[CrossRef](#)] [[PubMed](#)]
4. Yu, H.; Shen, X.; Chen, H.; Dong, H.; Zhang, L.; Yuan, T.; Zhang, D.; Shang, X.; Tan, Q.; Liu, J.; et al. Analysis of heavy metal content in *Lentinula edodes* and the main influencing factors. *Food Control* **2021**, *130*, 108198–108205. [[CrossRef](#)]
5. Shi, D.; Yin, C.; Fan, X.; Yao, F.; Qiao, Y.; Xue, S.; Lu, Q.; Feng, C.; Meng, J.; Gao, H. Effects of ultrasound and gamma irradiation on quality maintenance of fresh *Lentinula edodes* during cold storage. *Food Chem.* **2022**, *373*, 131478. [[CrossRef](#)]
6. Chen, Y.-h.; Chen, J. Optimization of extraction conditions for polysaccharides from *Collybia albuminosa* via response surface methodology. *Mod. Food Sci. Technol.* **2012**, *28*, 541.
7. Peng, X.R.; Su, H.G.; Liu, J.H.; Huang, Y.J.; Yang, X.Z.; Li, Z.R.; Zhou, L.; Qiu, M.H. C30 and C31 triterpenoids and triterpene sugar esters with cytotoxic activities from edible mushroom *Fomitopsis pinicola* (Sw. Ex Fr.) Krast. *J. Agric. Food. Chem.* **2019**, *67*, 10330–10341. [[CrossRef](#)]
8. Ying, Y.M.; Yu, H.F.; Tong, C.P.; Shan, W.G.; Zhan, Z.J. Spiroinonotsuoxotriols A and B, two highly rearranged triterpenoids from *Inonotus obliquus*. *Org. Lett.* **2020**, *22*, 3377–3380. [[CrossRef](#)]
9. Yu, J.; Xiang, J.Y.; Xiang, H.; Xie, Q. Cecal butyrate (Not Propionate) was connected with metabolism-related chemicals of mice, based on the different effects of the two *Inonotus obliquus* extracts on obesity and their mechanisms. *ACS Omega* **2020**, *5*, 16690–16700. [[CrossRef](#)]
10. Li, Y.-T.; Zhang, Z.; Feng, Y.; Cheng, Y.; Li, S.; Li, C.; Tian, L.-W. Cardioprotective 22-hydroxy lanostane triterpenoids from the fruiting bodies of *Phellinus igniarius*. *Phytochemistry* **2021**, *191*, 112907–112914. [[CrossRef](#)]
11. Cao, Y.; Liu, Y.; Wang, G.; Wang, W.; Li, Y.; Xuan, L. Styryl pyranones with apoptosis activities from the sporocarps of *Phellinus igniarius*. *Phytochem. Lett.* **2021**, *44*, 154–159. [[CrossRef](#)]
12. Shao, W.; Xiao, C.; Yong, T.; Zhang, Y.; Hu, H.; Xie, T.; Liu, R.; Huang, L.; Li, X.; Xie, Y.; et al. A polysaccharide isolated from *Ganoderma lucidum* ameliorates hyperglycemia through modulating gut microbiota in type 2 diabetic mice. *Int. J. Biol. Macromol.* **2022**, *197*, 23–38. [[CrossRef](#)] [[PubMed](#)]
13. Wen, L.; Sheng, Z.; Wang, J.; Jiang, Y.; Yang, B. Structure of water-soluble polysaccharides in spore of *Ganoderma lucidum* and their anti-inflammatory activity. *Food Chem.* **2022**, *373*, 131374. [[CrossRef](#)] [[PubMed](#)]
14. Han, W.; Chen, H.; Zhou, L.; Zou, H.; Luo, X.; Sun, B.; Zhuang, X. Polysaccharides from *Ganoderma sinense*—rice bran fermentation products and their anti-tumor activities on non-small-cell lung cancer. *BMC Complementary Med. Ther.* **2021**, *21*, 169–179. [[CrossRef](#)]
15. Teseo, S.; Houot, B.; Yang, K.; Monnier, V.; Liu, G.; Tricoire, H. *G. sinense* and *P. notoginseng* extracts improve healthspan of aging flies and provide protection in a huntington disease model. *Aging Dis.* **2021**, *12*, 425–440. [[CrossRef](#)]

16. Ahmad, R.; Riaz, M.; Khan, A.; Aljamea, A.; Algheryafi, M.; Sewaket, D.; Alqathama, A. *Ganoderma lucidum* (Reishi) an edible mushroom; a comprehensive and critical review of its nutritional, cosmeceutical, mycochemical, pharmacological, clinical, and toxicological properties. *Phytother. Res.* **2021**, *35*, 6030–6062. [[CrossRef](#)]
17. Zeng, M.; Qi, L.; Guo, Y.; Zhu, X.; Tang, X.; Yong, T.; Xie, Y.; Wu, Q.; Zhang, M.; Chen, D. Long-term administration of triterpenoids from *Ganoderma lucidum* mitigates age-associated brain physiological decline via regulating sphingolipid metabolism and enhancing autophagy in Mice. *Front. Aging Neurosci.* **2021**, *13*, 628860–628881. [[CrossRef](#)] [[PubMed](#)]
18. Xu, J.; Xiao, C.; Xu, H.; Yang, S.; Chen, Z.; Wang, H.; Zheng, B.; Mao, B.; Wu, X. Anti-inflammatory effects of *Ganoderma lucidum* sterols via attenuation of the p38 MAPK and NF- κ B pathways in LPS-induced RAW 264.7 macrophages. *Food Chem. Toxicol.* **2021**, *150*, 112073–112082. [[CrossRef](#)]
19. Shao, C.S.; Feng, N.; Zhou, S.; Zheng, X.X.; Wang, P.; Zhang, J.S.; Huang, Q. Ganoderic acid T improves the radiosensitivity of HeLa cells via converting apoptosis to necroptosis. *Toxicol. Res.* **2021**, *10*, 531–541. [[CrossRef](#)]
20. Kou, R.W.; Gao, Y.Q.; Xia, B.; Wang, J.Y.; Liu, X.N.; Tang, J.J.; Yin, X.; Gao, J.M. Ganoderterpene A, a New Triterpenoid from *Ganoderma lucidum*, Attenuates LPS-Induced Inflammation and Apoptosis via Suppressing MAPK and TLR-4/NF-kappaB Pathways in BV-2 Cells. *J. Agric. Food. Chem.* **2021**, *69*, 12730–12740. [[CrossRef](#)]
21. Wang, Y.-Q.; Wang, N.-X.; Luo, Y.; Yu, C.-Y.; Xiao, J.-H. Ganoderal A effectively induces osteogenic differentiation of human amniotic mesenchymal stem cells via cross-talk between Wnt/ β -catenin and BMP/SMAD signaling pathways. *Biomed. Pharmacother.* **2020**, *123*, 109807–109817. [[CrossRef](#)] [[PubMed](#)]
22. Chen, Y.; Gao, J.; Chen, Q.; Liu, W.; Qi, Y.; Aisa, H.A.; Yuan, T. Applanic acids A-C, three new highly oxygenated lanostane triterpenoids from the fruiting bodies of *Ganoderma applanatum*. *Nat. Prod. Res.* **2020**, *35*, 3918–3924. [[CrossRef](#)] [[PubMed](#)]
23. Song, X.; Cui, W.; Gao, Z.; Zhang, J.; Jia, L. Structural characterization and amelioration of sulfated polysaccharides from *Ganoderma applanatum* residue against CCl₄-induced hepatotoxicity. *Int. Immunopharmacol.* **2021**, *96*, 107554–107563. [[CrossRef](#)]
24. Mfopa, A.; Mediesse, F.K.; Mvongo, C.; Nkoubatchoundjwen, S.; Lum, A.A.; Sobngwi, E.; Kamgang, R.; Boudjeko, T. Antidyslipidemic potential of water-soluble polysaccharides of *Ganoderma applanatum* in MACAPOS-2-induced obese rats. *Evid. Based Complement. Alternat. Med.* **2021**, *2021*, 2452057. [[CrossRef](#)] [[PubMed](#)]
25. Hossen, S.M.M.; Islam, M.J.; Hossain, M.R.; Barua, A.; Uddin, M.G.; Emon, N.U. CNS anti-depressant, anxiolytic and analgesic effects of *Ganoderma applanatum* (mushroom) along with ligand-receptor binding screening provide new insights: Multi-disciplinary approaches. *Biochem. Biophys. Rep.* **2021**, *27*, 101062. [[CrossRef](#)]
26. Hossain, M.S.; Barua, A.; Tanim, M.A.H.; Hasan, M.S.; Islam, M.J.; Hossain, R.M.; Emon, N.U.; Hossen, S.M.M. *Ganoderma applanatum* mushroom provides new insights into the management of diabetes mellitus, hyperlipidemia, and hepatic degeneration: A comprehensive analysis. *Food Sci. Nutr.* **2021**, *9*, 4364–4374. [[CrossRef](#)] [[PubMed](#)]
27. Su, H.G.; Wang, Q.; Zhou, L.; Peng, X.R.; Xiong, W.Y.; Qiu, M.H. Functional triterpenoids from medicinal fungi *Ganoderma applanatum*: A continuous search for antiadipogenic agents. *Bioorg. Chem.* **2021**, *112*, 104977–104986. [[CrossRef](#)]
28. Su, H.G.; Wang, Q.; Zhou, L.; Peng, X.R.; Xiong, W.Y.; Qiu, M.H. Highly oxygenated lanostane triterpenoids from *Ganoderma applanatum* as a class of agents for inhibiting lipid accumulation in adipocytes. *Bioorg. Chem.* **2020**, *104*, 104263–104276. [[CrossRef](#)]
29. Peng, X.R.; Wang, Q.; Wang, H.R.; Hu, K.; Xiong, W.Y.; Qiu, M.H. FPR2-based anti-inflammatory and anti-lipogenesis activities of novel meroterpenoid dimers from *Ganoderma*. *Bioorg. Chem.* **2021**, *116*, 105338–105348. [[CrossRef](#)]
30. Peng, X.; Su, H.; Wang, H.; Hu, G.; Hu, K.; Zhou, L.; Qiu, M. Applanmerotic acids A and B, two meroterpenoid dimers with an unprecedented polycyclic skeleton from *Ganoderma applanatum* that inhibit formyl peptide receptor 2. *Org. Chem. Front.* **2021**, *8*, 3381–3389. [[CrossRef](#)]
31. Lee, S.Y.; Kim, J.S.; Lee, S.; Kang, S.S. Polyoxygenated ergostane-type sterols from the liquid culture of *Ganoderma applanatum*. *Nat. Prod. Res.* **2011**, *25*, 1304–1311. [[CrossRef](#)]
32. Peng, X.; Liu, J.; Xia, J.; Wang, C.; Li, X.; Deng, Y.; Bao, N.; Zhang, Z.; Qiu, M. Lanostane triterpenoids from *Ganoderma hainanense* J. D. Zhao. *Phytochemistry* **2015**, *114*, 137–145. [[CrossRef](#)]
33. Wang, Q.; Mu, R.F.; Liu, X.; Zhou, H.M.; Xu, Y.H.; Qin, W.Y.; Yang, C.R.; Wang, L.B.; Li, H.Z.; Xiong, W.Y. Steaming changes the composition of saponins of *Panax notoginseng* (Burk.) F.H. Chen that function in treatment of hyperlipidemia and obesity. *J. Agric. Food. Chem.* **2020**, *68*, 4865–4875. [[CrossRef](#)] [[PubMed](#)]
34. Pu, D.; Li, X.; Lin, J.; Zhang, R.; Luo, T.; Wang, Y.; Gao, J.; Zeb, M.A.; Zhang, X.; Li, X.; et al. Triterpenoids from *Ganoderma gibbosum*: A class of sensitizers of FLC-Resistant candida albicans to fluconazole. *J. Nat. Prod.* **2019**, *82*, 2067–2077. [[CrossRef](#)] [[PubMed](#)]
35. Pu, D.-B.; Zheng, X.; Gao, J.-B.; Zhang, X.-J.; Qi, Y.; Li, X.-S.; Wang, Y.-M.; Li, X.-N.; Li, X.-L.; Wan, C.-P.; et al. Highly oxygenated lanostane-type triterpenoids and their bioactivity from the fruiting body of *Ganoderma gibbosum*. *Fitoterapia* **2017**, *119*, 1–7. [[CrossRef](#)] [[PubMed](#)]
36. Peng, X.; Li, L.; Dong, J.; Lu, S.; Lu, J.; Li, X.; Zhou, L.; Qiu, M. Lanostane-type triterpenoids from the fruiting bodies of *Ganoderma applanatum*. *Phytochemistry* **2019**, *157*, 103–110. [[CrossRef](#)] [[PubMed](#)]
37. Li, L.; Peng, X.-R.; Dong, J.-R.; Lu, S.-Y.; Li, X.-N.; Zhou, L.; Qiu, M.-H. Rearranged lanostane-type triterpenoids with anti-hepatic fibrosis activities from *Ganoderma applanatum*. *RSC Adv.* **2018**, *8*, 31287–31295. [[CrossRef](#)]
38. Yoshikawa, K.; Nishimura, N.; Bando, S.; Arihara, S.; Matsumura, E.; Katayama, S. New lanostanoids, elfvingic acids A-H, from the fruit body of *Elfoingia applanata*. *J. Nat. Prod.* **2002**, *65*, 548–552. [[CrossRef](#)]